

Modeling of delays in PKPD: classical approaches and a tutorial for delay differential equations

Gilbert Koch · Wojciech Krzyzanski ·
Juan Jose Pérez-Ruixo · Johannes Schropp

Received: 23 January 2014 / Accepted: 26 June 2014 / Published online: 21 August 2014
© Springer Science+Business Media New York 2014

Abstract In pharmacokinetics/pharmacodynamics (PKPD) the measured response is often delayed relative to drug administration, individuals in a population have a certain lifespan until they mature or the change of biomarkers does not immediately affects the primary endpoint. The classical approach in PKPD is to apply transit compartment models (TCM) based on ordinary differential equations to handle such delays. However, an alternative approach to deal with delays are delay differential equations (DDE). DDEs feature additional flexibility and properties, realize more complex dynamics and can complementary be used together with TCMs. We introduce several delay based PKPD models and investigate mathematical properties of general DDE based models, which serve as subunits in order to build larger PKPD models. Finally, we review current PKPD software with respect to the implementation of DDEs for PKPD analysis.

Keywords Delay · Lifespan · Delay differential equation · Transit compartment model

Electronic supplementary material The online version of this article (doi:10.1007/s10928-014-9368-y) contains supplementary material, which is available to authorized users.

G. Koch (✉) · W. Krzyzanski
Department of Pharmaceutical Sciences, State University of
New York at Buffalo, 403 Kapoor Hall, Buffalo, NY 14214,
USA
e-mail: gilbertk@buffalo.edu

J. J. Pérez-Ruixo
Pharmacokinetics and Drug Metabolism, AMGEN. Puzol,
Valencia, Spain

J. Schropp
Department of Mathematics and Statistics, Universität Konstanz,
PO Box 195, 78457 Konstanz, Germany

Introduction

Mathematical pharmacokinetic/pharmacodynamic (PKPD) models describe the pharmacological effect on a measurable response, therapeutic or toxic, caused by drug administration, where in general drug concentration is measured in plasma and the response is a biomarker. The field of PKPD modeling has evolved from focusing on empirical description of the data into a mechanistic, biological based, science that integrates generated data and quantitatively supports the decision making process at all stages of drug development. A PKPD model could roughly be categorized in four structural parts (see Mager et al. [1] and Danhof et al. [2]):

- (1) Pharmacokinetic model: Describes the drug concentration in plasma.
- (2) Receptor/target-concentration model: Describes the binding of drug molecules to the receptor/target.
- (3) Transduction model: Describes a cascade of processes that govern the course of pharmacological response after drug-induced target activation.
- (4) Disease model: Describes the disease development.

In general the administration of a drug does not immediately lead to an observed response, because mechanistic events could occur in (1)–(4). For example:

- (i) For oral (p.o.) drug administration, the drug concentration measured in plasma may be delayed compared to the dosing time points, see [3, 4].
- (ii) The available drug concentration at the effect/target/receptor side (which in most cases is not measurable) could be delayed relative to drug concentration in plasma, compare [5].
- (iii) The modulation at the target site by the drug may cause a delay of the measurable biomarker, see [6].

- (iv) The change in biomarkers does not immediately lead to changes in clinical endpoints, see [7].

Generally speaking, in biological systems delays occur when the change in time of the variable of interest (e.g. signal intensity, drug concentration, cell count, tumor size, etc.) depends on past or history of one or more variables controlling the production or elimination processes [8]. Examples of systems with delays are maturation of blood cells, neurophysiology of retina, incubation times in epidemic models, neuron interaction model, chemostat models etc.

Traditionally, transit compartment models (TCMs) are applied to describe delays in PKPD because they capture a variety of data quite well, either from the data-driven or semi-mechanistical point of view. Such models are cascades of consecutive states and could be motivated by the pathway of signal transduction, see [6, 9]. Mathematically, these models are based on ordinary differential equations (ODEs). In TCMs the delay is implicitly given via the ratio of the number of compartments and the transit rate.

An alternative approach to handle delays are delay differential equations (DDEs), see e.g. [10]. Such equations consist of an explicit delay parameter and at least one single state to describe a delay. Notably, DDEs are an extension of ODEs and therefore, DDEs do not exclude the use of TCMs. Moreover, DDEs are a more flexible mathematical tool than ODEs and the dynamics of DDEs could realize more complex behavior than its ODE counterpart.

In this work, we review several PKPD approaches dealing with delays. In section “[Transit compartment models](#)” we shortly present the standard approaches to describe delays based on TCMs. Section “[Lifespan models](#)” deals with lifespan models (LSM) for population maturation modeling. In this concept, individuals entering a population have a certain lifespan and after expiration, the individuals leave the population. In section “[Characterization of four basic models with an explicit delay parameter](#)” we apply LSMs as subunits in more complex PKPD models and present a rough categorization of four basic model structures. This provides a link to general DDEs which are presented in section “[Delay differential equations and mathematical properties](#)”. It will turn out that a frequently used special sub-category of DDEs in lifespan modeling has an important property which could be exploited for implementation in current PKPD software. In section “[Implementation of delay differential equations](#)” we focus on the implementation of DDE based models in PKPD software and therefore investigate different PKPD software functionalities.

Finally, we have to mention a formalistic convention. In PKPD modeling the terms delay, lag-time and lifespan are sometimes interchangeably used which could lead to confusion. In this work, the term lifespan describes the lifespan

of individuals in a population. In contrast, a delay is a general term to describe any kind of retardation between a signal and the observed response. The term lag-time describes the delayed absorption in PK. Additionally, a remark about the presented mathematical notation is necessary. It is apparent in PKPD that the time-dependency of the states and sometimes also the initial values are neglected. When working with DDEs such a loose notation may cause confusion because states could also depend on the past $t - T$. Further the initial conditions are no longer just values at a specific time point but time-dependent functions. Therefore, a precise notation is necessary when working with DDEs.

Transit compartment models

The ordinary differential equations starting at $t_0 = 0$ for the transit compartment model (TCM) with inflow $k_{in}(t)$ are for $t \geq 0$ as follows:

$$\frac{d}{dt}x_1(t) = k_{in}(t) - kx_1(t), \quad x_1(0) = x_1^0 \geq 0 \quad (1)$$

$$\frac{d}{dt}x_2(t) = kx_1(t) - kx_2(t), \quad x_2(0) = x_2^0 \geq 0 \quad (2)$$

\vdots

$$\frac{d}{dt}x_n(t) = kx_{n-1}(t) - kx_n(t), \quad x_n(0) = x_n^0 \geq 0 \quad (3)$$

where $k > 0$ is the transit rate between the compartments and the integer n denotes the number of compartments. Assuming that the inflow $k_{in}(t)$ has a steady state, i.e.

$$\lim_{t \rightarrow \infty} k_{in}(t) = k_{in}^* \geq 0, \quad (4)$$

the baseline condition for Eqs. (1)–(3) reads

$$x_i^0 = x_i^* = \frac{k_{in}^*}{k} \quad \text{for } i = 1, \dots, n.$$

A physiological motivation for TCMs are signal transduction pathways, compare e.g. [6, 9].

A delay produced by a single compartment could be interpreted as the average time $\frac{1}{k}$ an individual (e.g. cell or molecule) resides in that single compartment. Hence, the overall average time an individual stays in the whole transit cascade is implicitly given by

$$MTT = \frac{n}{k}$$

and called the mean transit time. A common choice is to fix n a-priori and to estimate k in a fitting process. Then the MTT is calculated as a secondary parameter. However, we remark that in special situations the number of compartments was also optimized, see [3] or [11].

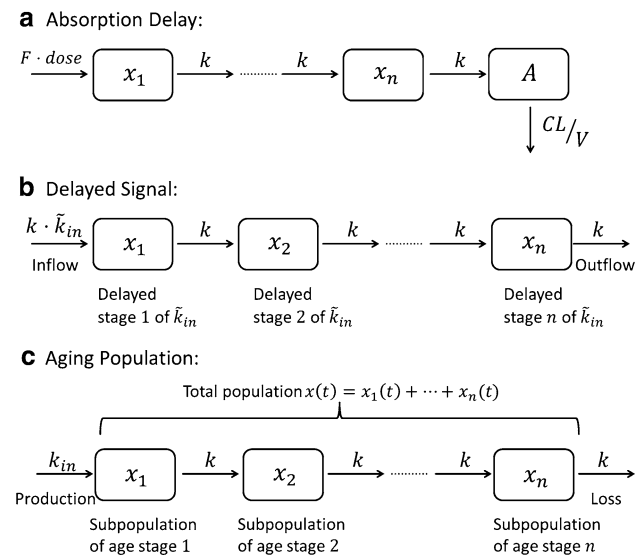


Fig. 1 The upper scheme **a** visualizes an absorption delay, the middle scheme **b** shows the use of a TCM to delay a signal and the lower scheme **c** presents the application of a TCM to describe an aging population

TCMs are traditionally applied to account for an absorption delay, to produce a delayed signal and to describe an aging population.

Transit compartments for absorption delay

The absorption delay is the time necessary for a drug molecule to reach the systematic circulation from the depot site (e.g. gastro-intestinal track, intraperitoneal cavity or subcutaneous tissue) following drug administration. The delay is determined by complex processes involving transport and metabolism frequently resulting in a drug fractional bioavailability [4]. It is worth mentioning that already in 1971, Bischoff et al. [12] proposed a physiologically based pharmacokinetic model where delays in drug distribution are modeled with a TCM. In [3, 13, 14] TCMs have been introduced to describe absorption delays. In its simplest form a TCM for an absorption delay consists of a series of transit compartments feeding into a central compartment representing circulating plasma, see Fig. 1a and reads:

$$\frac{d}{dt}x_1(t) = -kx_1(t), \quad x_1(0) = F \text{dose} \quad (5)$$

$$\frac{d}{dt}x_i(t) = k(x_{i-1}(t) - x_i(t)), \quad x_i(0) = 0 \quad \text{for } i = 2, \dots, n \quad (6)$$

$$\frac{d}{dt}A(t) = kx_n(t) - \frac{CL}{V}A(t), \quad A(0) = 0 \quad (7)$$

where F is the bioavailability, V is the central compartment volume, CL denotes the systematic clearance and $A(t)$ is

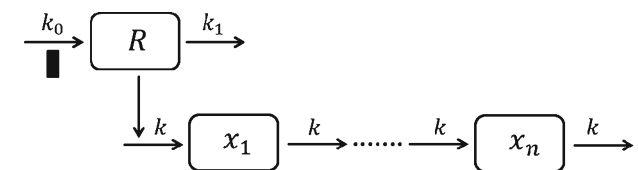
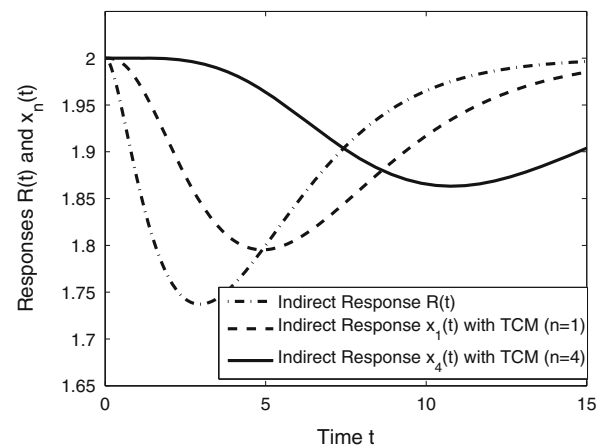


Fig. 2 Simulated time course of models Eq. (10)–(13). The PK parameter are $k_{el} = 0.5$, $k_a = 0.7$ and $V = 1$ with $\text{dose} = 10$. The PD parameters are $I_{max} = 0.5$, $IC_{50} = 10$, $R^0 = 2$, $k_0 = 2$, $k_1 = 1$ and $k = 0.5$

the drug amount in the central compartment. In the context of the absorption process, MTT is interpreted as a mean absorption delay and serves as an equivalent of the absorption rate.

Use of transit compartments to produce a delayed signal

The standard form of a TCM to delay a signal $\widetilde{k}_{in}(t)$ (see [6]) with $\lim_{t \rightarrow \infty} \widetilde{k}_{in}(t) = k_{in}^*$ reads

$$\frac{d}{dt}x_1(t) = k(\widetilde{k}_{in}(t) - x_1(t)), \quad x_1(0) = x_1^0 \quad (8)$$

$$\frac{d}{dt}x_i(t) = k(x_{i-1}(t) - x_i(t)), \quad x_i(0) = x_i^0 \quad \text{for } i = 2, \dots, n \quad (9)$$

where the last compartment $x_n(t)$ is used to describe the delayed signal. The steady states of Eqs. (8)–(9) read $x_i^* = k_{in}^*$ for $i = 1, \dots, n$. In Fig. 1b a schematic of Eqs. (8)–(9) is presented.

Sheiner et al. [5] applied a hypothetical effect compartment to delay the access of the drug concentration to the hypothetical biophase. Prominent PKPD examples where signals are delayed are [15] (delayed effect of methotrexate with $n = 4$), [16] (delayed cytokine production in arthritic rats with large n 's) and [17] where a TCM is used to describe a feedback on proliferating cells for chemotherapy-induced myelosuppression.

Delayed indirect response

We apply two models (one without and one with a TCM) to visualize their capability to capture a delay. The PK is described by the Bateman function

$$c(t) = \frac{\text{dose}}{V} \frac{k_a}{k_a - k_{el}} (\exp(-k_{el}t) - \exp(-k_a t))$$

where k_a is the absorption rate, k_{el} the elimination rate and V the volume of distribution. Often a drug $c(t)$ stimulates or inhibits factors indirectly which then finally control the response $R(t)$, see [18]. We consider the inhibition of a response $R(t)$ hovering in a baseline $R^0 = \lim_{t \rightarrow \infty} R(t) = R^*$ by

$$I(t) = \frac{I_{\max} c(t)}{IC_{50} + c(t)}$$

where $0 < I_{\max} \leq 1$ is the maximal inhibition and $IC_{50} > 0$ the drug concentration necessary to produce half-maximal inhibition. The indirect response (IDR) model I reads

$$\frac{d}{dt} R(t) = k_0(1 - I(t)) - k_1 R(t), \quad R(0) = R^0 = \frac{k_0}{k_1} \quad (10)$$

where $k_0 > 0$ is the zero order production rate and $k_1 > 0$ the first order loss rate. Please note that Eq. (10) is a TCM with $n = 1$. Now let the inflow be $\widetilde{k}_{in}(t) = R(t)$ and coupling Eq. (10) with the TCM Eqs. (8)–(9) to delay $R(t)$ results in

$$\frac{d}{dt} R(t) = k_0(1 - I(t)) - k_1 R(t), \quad R(0) = \frac{k_0}{k_1} \quad (11)$$

$$\frac{d}{dt} x_1(t) = k(R(t) - x_1(t)), \quad x_1(0) = \frac{k_0}{k_1} \quad (12)$$

$$\frac{d}{dt} x_i(t) = k(x_{i-1}(t) - x_i(t)), \quad x_i(0) = \frac{k_0}{k_1} \quad \text{for } i = 2, \dots, n \quad (13)$$

where $x_n(t)$ is the delayed response of $R(t)$. In Figure 2 we present the responses of the models Eq. (10) and Eqs. (11)–(13). Please note that for increasing n the sharpness of the delayed signal diminish as explained in [9]. Including a power coefficient $\gamma > 0$ in the last compartment of the TCM

$$\frac{d}{dt} x_n(t) = k(x_{n-1}^\gamma(t) - x_n(t))$$

allows to amplify or suppress the profile of $x_n(t)$, see [9].

Use of transit compartments to describe an aging population

Another application of TCMs is to describe an aging population (e.g. of cells). Then the compartments $x_i(t)$

describe subpopulations of different age stages of the total population $x_1(t) + \dots + x_n(t)$. From the last stage $x_n(t)$ the individuals have to leave the population. In this context the mean transit time MTT describes the mean lifespan of the individuals. In Fig. 1c we present the schematic of a TCM to describe an aging population.

Harker et al. [19], and later Wang et al. [20], applied TCMs to describe the platelet maturation process where the i -th transit compartment represents a cell pool of age i/k . This concept was applied to describe the dynamics of red blood cells in healthy subjects [21], cancer patients receiving chemotherapy [22] and patients with chronic renal failure [23]. Simeoni et al. [24] presented a model for tumor growth and anticancer effects where the TCM describes the apoptosis of tumor cells attacked by a drug. In [25] two TCMs are applied to describe the aging process of megakaryocytes (first TCM) which mature into platelets (second TCM).

Lifespan models

Lifespan models are typically used to describe (cell-) populations where the individuals entering a population have a specific lifespan. After expiration of their lifespan the individuals have to leave the population. We distinguish between two kinds of lifespan models. First we present models where all individuals have the same lifespan, called a point distribution. Then we consider models with an arbitrary distributed lifespan, i.e. every individual has its own lifespan.

In general, a population $y(t)$ is controlled by production (birth or entry into the population) $k_{in}(t)$ and loss (death or exit from the population) $k_{out}(t)$. The typical form of a lifespan model for $y(t)$ starting at $t_0 = 0$ reads

$$\frac{d}{dt} y(t) = k_{in}(t) - k_{out}(t), \quad y(0) = y^0 \quad \text{for } t \geq 0 \quad (14)$$

where the lifespan is included by different designs of the loss term $k_{out}(t)$.

Lifespan models with a point distribution

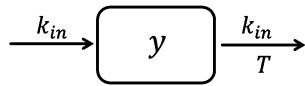
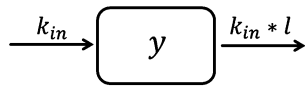
It is assumed that every individual in the population $y(t)$ has the same lifespan $T > 0$, called a point distribution. Then the outflow from state y at time t is equal to the inflow at time $t - T$ and therefore,

$$k_{out}(t) = k_{in}(t - T) \quad \text{for } t \geq 0. \quad (15)$$

Hence, the basic lifespan model (LSM) reads

$$\frac{d}{dt} y(t) = k_{in}(t) - k_{in}(t - T), \quad y(0) = y^0, \quad (16)$$

see Fig. 3a for a schematic. Now k_{in} also has to be defined for the past $-T \leq t < 0$. Models of type Eq. (16) are used

a Lifespan model (LSM) with point distribution**b** Lifespan model (DLSM) with arbitrary distribution**Fig. 3** In the upper panel (a) the lifespan model Eq. (16) with a point distributed lifespan T is shown and in the lower panel (b) the distributed lifespan model Eq. (43) is presented

later in this manuscript as sub-units to build more complex structures consisting of a general delay which opens the route to delay differential equations.

Lifespan-based population with baseline condition

In a lifespan-based population the initial value y^0 can be chosen based on a relationship between the production of individuals in the past and the number of subjects born at time $t = 0$. For that purpose we consider these individuals to form a cohort (a population of subjects of the same age). For a cohort there is no production of new individuals ($k_{in}(t) = 0$ for $t > 0$), and the elimination is determined by their lifespan [26]. Since all individuals in the cohort have the same lifespan T , $y(T) = 0$. Integration of Eq. (16) over time interval $[0, T]$ yields:

$$y^0 = \int_{-T}^0 k_{in}(s) ds. \quad (17)$$

The integral solution of model Eqs. (16)–(17) is

$$y(t) = \int_{t-T}^t k_{in}(s) ds = \int_0^T k_{in}(t-s) ds \quad \text{for } t \geq 0. \quad (18)$$

Assuming Eq. (4), the steady state reads

$$y^* = \lim_{t \rightarrow \infty} y(t) = k_{in}^* T. \quad (19)$$

With a constant production in the past corresponding to the steady state

$$k_{in}(t) = k_{in}^* \quad \text{for } t < 0 \quad (20)$$

the initial value Eq. (17) reduces to

$$y^0 = k_{in}^* T$$

and therefore, we have the baseline condition

$$y^0 = y^* = k_{in}^* T. \quad (21)$$

Example 1: Basic lifespan model

Let us consider a one-compartment PK model

$$\frac{d}{dt} c(t) = -k_{el} c(t). \quad (22)$$

We set the past of the PK as

$$c(t) = \begin{cases} 0 & \text{for } t < 0 \\ c^0 \geq 0 & \text{for } t = 0 \end{cases}. \quad (23)$$

Let T_R be the lifespan of the individuals in a population R . The production is set in the context of indirect response and reads

$$k_{in}(t) = k_0 \left(1 + \frac{S_{max} c(t)}{SC_{50} + c(t)} \right) \quad \text{for } t \geq -T_R$$

where S_{max} is the maximal stimulation and SC_{50} is the concentration necessary to produce half-maximal effect. The basic LSM Eqs. (16)–(17), in this context also called lifespan indirect response model (LIDR), is

$$\begin{aligned} \frac{d}{dt} R(t) = & k_0 \left(1 + \frac{S_{max} c(t)}{SC_{50} + c(t)} \right) \\ & - k_0 \left(1 + \frac{S_{max} c(t - T_R)}{SC_{50} + c(t - T_R)} \right), \quad R(0) = k_0 T_R. \end{aligned} \quad (24)$$

In section “Implementation of delay differential equations”, model Eqs. (22)–(24) will be investigated in full detail.

Relationship between transit compartments and lifespan models with a point distribution

It turned out (see [27] or [28] for more details and a mathematical proof) that TCMs are related to lifespan models with a point distribution. Roughly summarized, let $MTT = n/k$ be fixed and consider the total sum of the compartments of Eqs. (1)–(3)

$$y_n(t) = x_1(t) + \dots + x_n(t).$$

If the number of compartments n tends to infinity, then

$$\lim_{n \rightarrow \infty} y_n(t) = y(t) \quad \text{for } t \geq 0$$

satisfies the equation

$$\frac{d}{dt} y(t) = k_{in}(t) - k_{in}(t - T), \quad y(0) = y^0 \quad \text{for } t \geq 0 \quad (25)$$

where $T = MTT$. Hence, TCMs could be considered as an approximation of LSMs.

Example 2: Lifespan based tumor growth model

An application of the presented relationship allows one to rewrite the PKPD tumor growth model from Simeoni et al. [24] with a lifespan model. The general structure of Simeoni's PKPD tumor growth model reads

$$\begin{aligned} \frac{d}{dt}p(t) &= g(\mu, p(t), d_1(t) + \dots + d_n(t)) - e(\kappa, c(t))p(t), \\ p(0) &= w_0 \end{aligned} \quad (26)$$

$$\frac{d}{dt}d_1(t) = e(\kappa, c(t))p(t) - kd_1(t), \quad d_1(0) = 0 \quad (27)$$

$$\frac{d}{dt}d_i(t) = k(d_{i-1}(t) - d_i(t)), \quad d_i(0) = 0 \quad \text{for } i = 2, \dots, n \quad (28)$$

$$w(t) = p(t) + d_1(t) + \dots + d_n(t) \quad (29)$$

where $p(t)$ denotes the proliferating cells and $d_1(t), \dots, d_n(t)$ the different apoptotic stages of tumor cells attacked by a drug. The total tumor weight $w(t)$ is the sum of proliferating cells $p(t)$ and the apoptotic cell population $d_1(t) + \dots + d_n(t)$ where the tumor weight is a surrogate of the total number of tumor cells. The growth mechanism is described by g and the drug effect term by e . The model parameters are μ (unperturbed tumor growth), κ (drug related parameters) and w_0 is the inoculated tumor weight.

Equations (27)–(28) are a TCM with inflow

$$k_{in}(t) = e(\kappa, c(t))p(t). \quad (30)$$

To describe the apoptotic cell population with an LSM we set

$$d(t) = d_1(t) + \dots + d_n(t)$$

and replace the TCM by a LSM due to the presented relationship. Using Eq. (30) this leads to

$$\begin{aligned} \frac{d}{dt}d(t) &= k_{in}(t) - k_{in}(t - T_d) \\ &= e(\kappa, c(t))p(t) - e(\kappa, c(t - T_d))p(t - T_d) \end{aligned}$$

completed by the initial condition $d(0) = 0$ and the past

$$e(\kappa, c(t))p(t) = 0 \quad \text{for } -T_d \leq t \leq 0 \quad (31)$$

where T_d is the lifespan of the apoptotic cells. In application to the analysis of xenograft data, Eq. (31) is fulfilled because no drug is administered before inoculation of tumor cells. Summarizing, the reformulation of model Eqs. (26)–(29) in the lifespan model context reads

$$\begin{aligned} \frac{d}{dt}p(t) &= g(\mu, p(t), d(t)) - e(\kappa, c(t))p(t), \\ p(t) &= \begin{cases} 0 & \text{for } -T_d \leq t < 0 \\ w_0 & \text{for } t = 0 \end{cases} \end{aligned} \quad (32)$$

Table 1 Parameter estimates for the lifespan based tumor growth model Eqs. (31)–(34) (Example 2) from BERKELEY MADONNA 8.3

Model parameter	Definition	Value
λ_0	Linear growth rate	1.97 E−1
λ_1	Exponential growth rate	2.44 E−1
w_0	Initial tumor weight	9.00 E−3
k_{pot}	Drug potency	7.00 E−3
T_d	Lifespan of apoptotic cells	3.31 E0

BERKELEY MADONNA does not provide CV% values

$$\begin{aligned} \frac{d}{dt}d(t) &= e(\kappa, c(t))p(t) - e(\kappa, c(t - T_d))p(t - T_d), \\ d(0) &= 0 \end{aligned} \quad (33)$$

$$w(t) = p(t) + d(t). \quad (34)$$

In the LSM formulation Eqs. (32)–(34) we have exactly two differential equations, one for the proliferating cells $p(t)$ and one governing the population of the apoptotic tumor cells $d(t)$. The lifespan T_d of the apoptotic tumor cells is now directly estimated from the data. The applied growth function with $\mu = (\lambda_0, \lambda_1)$ reads

$$g(\lambda_0, \lambda_1, p(t), d(t)) = \frac{2\lambda_0\lambda_1p(t)^2}{(\lambda_1 + 2\lambda_0p(t))(p(t) + d(t))} \quad (35)$$

where λ_0 is the exponential and λ_1 the linear growth rate. The drug effect is modeled with

$$e(k_{pot}, c(t)) = k_{pot}c(t)$$

where k_{pot} describes the potency of a drug. In “[Delay differential equations and mathematical properties](#)” section mathematical properties of Eqs. (32)–(34) are investigated and in “[Implementation of delay differential equations](#)” section the implementation in BERKELEY MADONNA is presented. In Fig. 4 the fit of data from [28] is shown and in Table 1 the parameter estimates are listed.

Lifespan models with a point distribution and a precursor

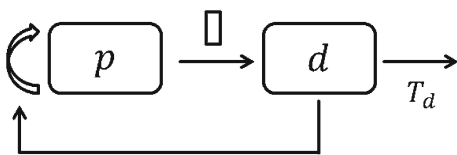
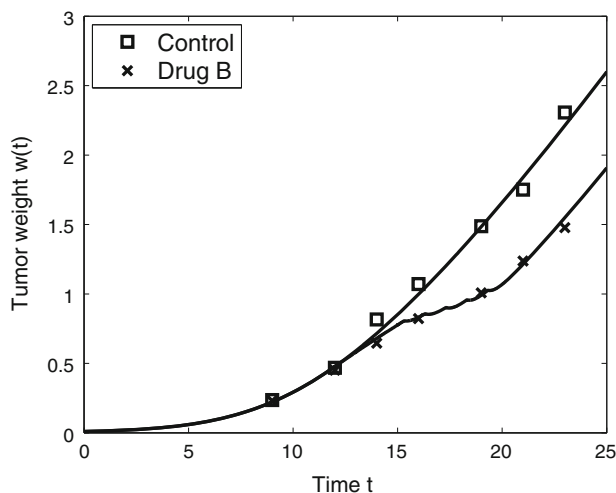
Additionally, we consider LSMs with a precursor population as introduced in [29]. Then Eq. (16) serves as a precursor population and individuals expiring from that population mature into a follow-up population $z(t)$. The precursor driven LSM reads

$$\frac{d}{dt}y(t) = k_{in}(t) - k_{in}(t - T_1), \quad y(0) = y^0 \quad (36)$$

$$\frac{d}{dt}z(t) = k_{in}(t - T_1) - k_{in}(t - T_1 - T_2), \quad z(0) = z^0 \quad (37)$$

Table 2 Parameter estimates for the precursor lifespan model for platelets Eqs. (39)–(41) (Example 3) from ADAPT 5

Model parameter	Definition	Value (CV%)
c_1	PK parameter	$3.31 \text{ E}1^a$
c_2	PK parameter	$9.26 \text{ E}0^a$
l_1	PK parameter	$1.49 \text{ E}-1^a$
l_2	PK parameter	$2.9 \text{ E}-2^a$
S_{max}	Maximal stimulation	$1.8 \text{ E}0^a$
SC_{50}	Concentration yielding half-maximal effect	$7.6 \text{ E}-3$ (40.5)
h	Hill coefficient	$6.31 \text{ E}-1$ (15.7)
k_{in}^0	Production rate	$4.06 \text{ E}-1$ (9.1)
T_P	Lifespan of platelets	$80.2 \text{ E}0$ (8.0)
T_R	Lifespan of megakaryocytes	$150.6 \text{ E}0$ (9.1)
η	Amplification factor	$6.1 \text{ E}0^a$

^a Fixed**Fig. 4** Fit of the tumor weight $w(t) = p(t) + d(t)$ from tumor growth model in the lifespan formulation Eqs. (31)–(34). The dose = 100 was orally administered at times $t=12, 13, 14, 15$ and 16 . Parameters are estimated with BERKELEY MADONNA and listed in Table 1

where T_1 is the lifespan of the precursor population and T_2 the lifespan of the follow-up population. If $z(t)$ is the only measured response, then only Eq. (37) needs to be solved because the right hand side is independent of $y(t)$. Similar to the basic LSM we obtain the integral solution representation

$$z(t) = \int_{t-T_1-T_2}^{t-T_1} k_{in}(s) ds = \int_0^{T_2} k_{in}(t - T_1 - s) ds$$

for $t \geq 0$. At the baseline condition we have

$$z^0 = z^* = k_{in}^* T_2. \quad (38)$$

Models of the form Eqs. (16), (20), (21) and Eqs. (36)–(38) were introduced by Krzyzanski and Jusko in 1999 [29] to PKPD modeling. They applied this approach to cell populations based on the indirect response context. Please note that the only difference between indirect response models and lifespan based models is that the loss rate is no longer a first-order process but the production rate delayed by lifespan. The pharmacology of the drug remained the same with the inhibitory or stimulatory effect described by the E_{max} model.

Example 3: Precursor lifespan model for platelets

In [29] the increase of megakaryocyte (no measurements) and platelet counts (measured) after administration of thrombopoietin (TPO) in cancer patients was modeled. The megakaryocytes form the precursor compartment $P(t)$ which are stimulated by TPO. Megakaryocyte maturation lasts for T_P hours and after that they yield platelets $R(t)$. The platelets stay in blood for T_R hours and are eliminated as a consequence of senescence or random destruction. The lifespan based indirect response (LIDR) model reads

$$\begin{aligned} \frac{d}{dt} R(t) &= \eta k_0 S(t - T_P) - \eta k_0 S(t - T_P - T_R), \\ R(0) &= \eta k_0 T_R \end{aligned} \quad (39)$$

where an amplification factor η for the production of the platelets was used. The stimulation was described by

$$S(t) = 1 + \frac{S_{max} c(t)^h}{SC_{50}^h + c(t)^h} \quad (40)$$

where $h > 0$ is the Hill coefficient. The PK was characterized by

$$c(t) = c_1 \exp(-l_1 t) + c_2 \exp(-l_2 t) \quad (41)$$

where c_1, c_2, l_1 and l_2 are the macro parameters of the biexponential function. For simplicity, we assumed there is no baseline endogenous TPO concentration in contrast to [29] and re-fitted the PK. In Fig. 5 the fit of the platelets is presented from the ADAPT 5 implementation (see section “Implementation of delay differential equations” for details). The estimates are listed in Table 2.

The precursor pool lifespan model for platelets has also been applied in the context of non-linear mixed effects models in order to characterize the PKPD properties of

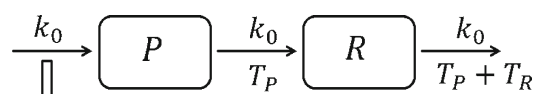
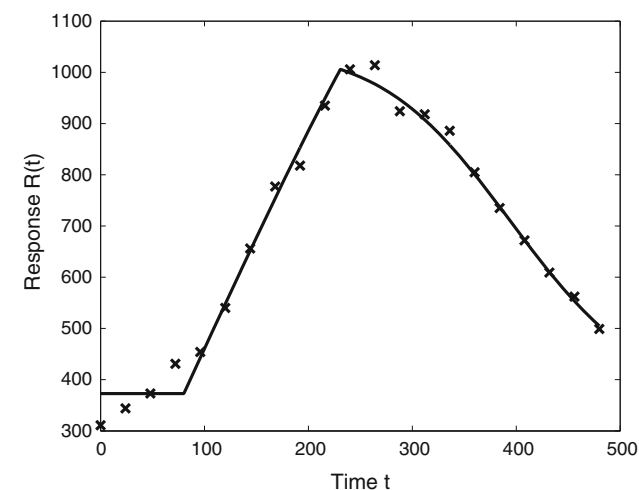


Fig. 5 Fit of the platelet count $R(t)$ with the precursor lifespan model for platelets Eqs. (39)–(40) in ADAPT 5. PD parameter estimates and fixed PK parameters are shown in Table 2

thrombopoietin receptor agonist and provides quantitative information for dosing regimen selection for Phase II study [30].

Lifespan models with a distributed lifespan

A realistic extension of the point distributed lifespan assumption is to consider an arbitrary distributed lifespan. Let \mathcal{T} be a random variable describing an arbitrary distribution of the lifespan τ of individuals based on a probability density function (PDF) $l(\tau)$. It is assumed that no negative lifespan exist, i.e. $l(\tau) = 0$ for $\tau < 0$. Let

$$T = E[T] = \int_0^{\infty} sl(s)ds$$

be the expected value. The lifespan distribution is included into the outflow term via the convolution operator

$$k_{out}(t) = \int_0^{\infty} k_{in}(t-\tau)l(\tau) d\tau = (k_{in} * l)(t) \quad (42)$$

see e.g. [31] or [32]. Typical distributions applied in survival analysis are e.g. Weibull or gamma, see [31, 33]. Note that Eq. (42) reduces to Eq. (15) in case of a point distribution $l(\tau) = \delta(\tau - T)$ where δ stands for the Dirac delta function. In Fig. 6 the difference between the Weibull distribution and a point distribution is visualized.

The distributed LSM (DLSM) reads

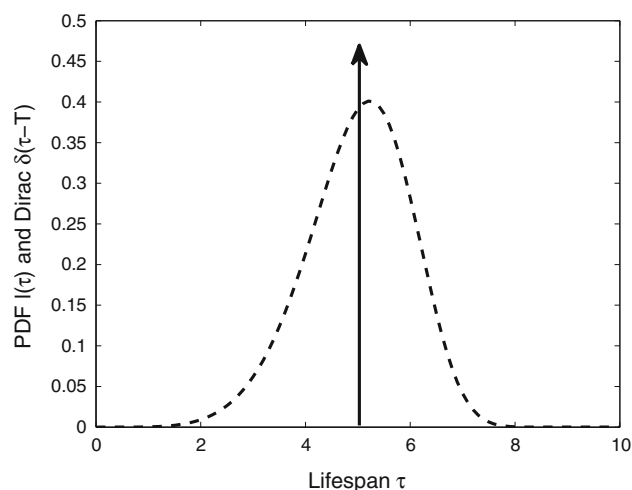


Fig. 6 The solid arrow indicates the point distribution described by the Dirac delta function $\delta(\tau - T)$ and the dashed curve is the probability density function $l(\tau)$ of the Weibull distribution. The parameters are mean $T = 5$ and variance $\sigma^2 = 1$. Note that the Weibull distribution is non-symmetric

$$\frac{d}{dt}y(t) = k_{in}(t) - (k_{in} * l)(t), \quad y(0) = y^0, \quad (43)$$

see Fig. 3b for a schematic. Again the initial value y^0 can be chosen based on the cohort argument, $k_{in}(t) = 0$ for $t > 0$. In the case of a distributed lifespan, all subjects in the cohort will eventually die, i.e. $\lim_{t \rightarrow \infty} y(t) = 0$. Integration of Eq. (43) over time interval $[0, \infty)$ yields

$$y^0 = \int_0^{\infty} l(x) \int_{-x}^0 k_{in}(s) ds dx, \quad (44)$$

see [33]. The solution of the DLSM Eqs. (43)–(44) reads

$$y(t) = \int_0^{\infty} \int_{t-x}^t k_{in}(s) ds l(x) dx \\ = \int_0^{\infty} (1 - L(s))k_{in}(t-s) ds \quad \text{for } t \geq 0 \quad (45)$$

where $L(\tau) = \int_0^{\tau} l(s)ds$ is the corresponding cumulative distribution function (CDF). Please note the difference in the two terms in Eq. (45). In the double integral the PDF $l(\tau)$ is used whereas in the single integral the CDF $L(\tau)$ is applied, see [33] for more details.

We remark that the inclusion of an arbitrary distribution could not be mimicked by a TCM of the standard form Eqs. (1)–(3). Also implementation of the DLSM Eqs. (43)–(44) is not straight forward, see [31] or [33] but is not topic of this work.

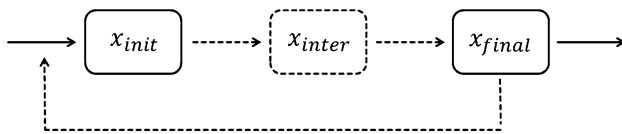


Fig. 7 The driver x_{init} governs a state x_{final} with one (or more) possible intermediate stages x_{inter} . From x_{final} a feedback to x_{init} could exist

Finally, we shortly mention some additional realistic extension of the presented lifespan concept. In [34] the lifespan distribution is also influenced by time t . In [32] this concept was applied to describe the lifespan of reticulocytes. However, also the drug itself could change the lifespan, see [35]. A review of this more sophisticated modeling of lifespans is out of scope of this manuscript and has been described in [36].

Characterization of four basic models with an explicit delay parameter

In this Section we characterize four basic models which could serve as modeling components for more complex systems. Conceptually, let x_{init} be a precursor/driver compartment which finally governs a state x_{final} perhaps using some subsequent intermediate stages. The compartment of x_{init} is coupled to one or more intermediate stages x_{inter} and from the intermediate stages to the x_{final} compartment. At least one process contains an explicit delay $T > 0$ and the PK acts at the x_{init} -compartment. From the x_{final} compartment there may or may not exist a feedback back to the x_{init} compartment, see Fig. 7.

In the case when no intermediate stages are present this concept reduces to four basic model classes. To keep the presentation as simple as possible we write $x_1 = x_{init}$, $x_2 = x_{final}$ and formulate model equations with time independent transit rates $k_1, k_2 > 0$.

Models with no feedback

Let $g(s(t), x_1(t))$ be the inflow into state $x_1(t)$ governed by a signal $s(t)$ with a possible dependency of $x_1(t)$.

Model A

State $x_1(t)$ consists of an inflow $g(s(t), x_1(t))$, a first order outflow $k_1 x_1(t)$ and drives the second state $x_2(t)$ described by model Eq. (16). The general structure of model A reads

$$\begin{aligned} \frac{d}{dt}x_1(t) &= g(s(t), x_1(t)) - k_1 x_1(t), \\ x_1(t) &= x_1^0(t) \text{ for } -T \leq t \leq 0 \end{aligned} \quad (46)$$

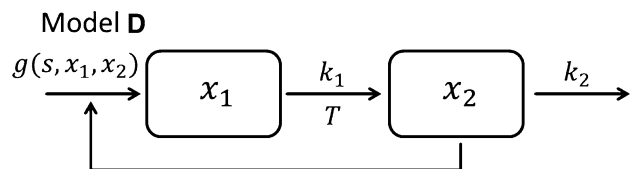
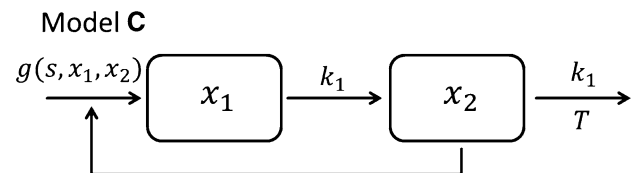
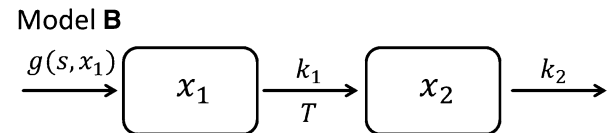
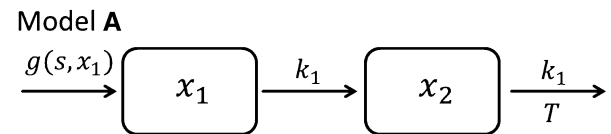


Fig. 8 Schematic visualization of the four models A Eqs. (46)–(47), B Eqs. (51)–(52), C Eqs. (54)–(55) and D Eqs. (56)–(57)

$$\frac{d}{dt}x_2(t) = k_1 x_1(t) - k_1 x_1(t - T), \quad x_2(0) = x_2^0. \quad (47)$$

The schematic of model A is presented in Fig. 8. Note that state $x_1(t)$ has a past given by the initial function $x_1^0(t)$ for $-T \leq t \leq 0$ whereas state $x_2(t)$ has no past but an initial value x_2^0 at time $t = 0$. Also note that Eq. (47) is independent of $x_2(t)$ and therefore, the solution of Eq. (47) could be computed a posteriori by pure integration. Implementation of model A in NONMEM has been reported in the literature [37] (see Example 4 below).

In [38, 39], model A appears as a sub-structure to describe the stimulatory effects of erythropoietin (EPO) on red blood cell (RBC) production. More precisely, $x_1(t)$ corresponds to a colony-forming unit CFU-E which drives the normoblasts, described by $x_2(t)$. Moreover, in [38, 39] reticulocytes and mature RBC are modeled with additional equations of the form Eq. (47).

Example 4: Lifespan indirect response model with a precursor pool

In [37] a lifespan indirect response model where the production rate in a precursor pool $P(t)$ is stimulated was developed. The lifespan of the population $R(t)$ is denoted by T_R and the model reads

$$\frac{d}{dt}c(t) = -k_{el}c(t), \quad c(0) = \frac{\text{dose}}{V} \quad (48)$$

$$\frac{d}{dt}P(t) = k_0 \left(1 + \frac{S_{max}c(t)}{SC_{50} + c(t)} \right) - k_1P(t), \quad (49)$$

$$P(t) = \frac{k_0}{k_1} \quad \text{for } -T_R \leq t \leq 0$$

$$\frac{d}{dt}R(t) = k_1P(t) - k_1P(t - T_R), \quad R(0) = k_0T_R. \quad (50)$$

Note that the PD part Eqs. (49)–(50) is model A where the stimulatory effect of PK $c(t)$ is described by the inflow $g(c(t)) = k_0 \left(1 + \frac{S_{max}c(t)}{SC_{50} + c(t)} \right)$.

In section “Implementation of delay differential equations” we discuss the implementation of Eqs. (48)–(50) in S-ADAPT. In Fig. 9 a fit is presented and the parameter estimates are listed in Table 3.

In contrast to model Eqs. (39)–(40) from Example 3, here the PD precursor Eq. (49) is delayed and not the PK. These type of models can also be applied to describe the tolerance effect due to depletion or blockage of the precursor pool, if the drug effect is on k_1 , as described in [40] for TCM. Then the stimulatory or inhibitory function should multiply the k_1 rate constant instead of k_0 , see [38, 39].

Model B

The development of state $x_2(t)$ is delayed with respect to the driver $x_1(t)$. With a delayed inflow $x_1(t - T)$ into $x_2(t)$ we obtain model B:

$$\frac{d}{dt}x_1(t) = g(s(t), x_1(t)) - k_1x_1(t), \quad (51)$$

$$x_1(t) = x_1^0(t) \quad \text{for } -T \leq t \leq 0$$

$$\frac{d}{dt}x_2(t) = k_1x_1(t - T) - k_2x_2(t), \quad x_2(0) = x_2^0. \quad (52)$$

In Eq. (52) inflow $k_1x_1(t - T)$ is responsible for the delay of $x_2(t)$ due to $x_1(t)$. For the schematic of model B see Fig. 8.

From the mechanistic point of view the delayed inflow into the x_2 -compartment in Eq. (52) could be explained by a lifespan equation (16) with inflow $k_{in}(t) = k_1x_1(t)$. More precisely, by adding

$$\frac{d}{dt}y(t) = k_1x_1(t) - k_1x_1(t - T), \quad y(0) = y^0 \quad (53)$$

to model B Eqs. (51)–(52). Hence, Eqs. (51)–(53) are a combination of models A and B. At the end of this Section we present in Example 6 a PKPD model where such a combined structure of models A and B is applied to

Table 3 Parameter estimates for the lifespan indirect response model with a precursor pool Eqs. (48)–(50) (Example 4) from S-ADAPT

Model parameter	Definition	Value (CV%)
k_{el}	Drug elimination rate	0.25 E0 ^a
V	Volume of distribution	1 E0 ^a
S_{max}	Maximal stimulation	86.7 E0 (16.8)
SC_{50}	Concentration yielding half-maximal effect	9.88 E0 (7.06)
k_0	Production rate constant for precursor	3.14 E−1(12.7)
k_1	Loss rate constant for precursor	5.00 E−3 (4.75)
T_R	Lifespan	33.7 E0 (8.33)

^a Fixed

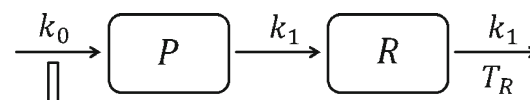
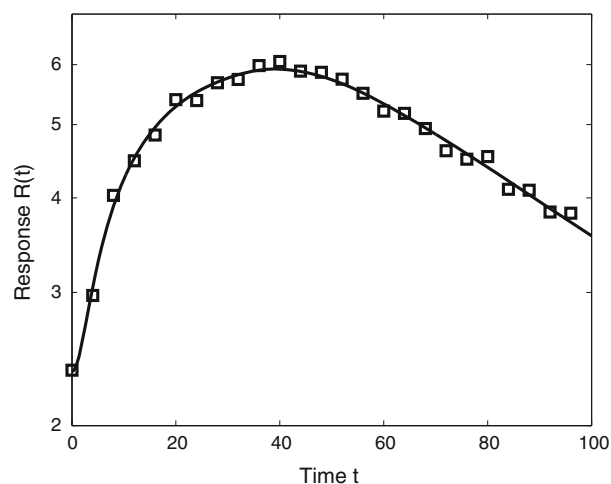


Fig. 9 Fit of log-transformed data with the lifespan indirect response model with precursor pool Eqs. (48)–(50) in S-ADAPT. A single dose = 1000 was intravenous administered at time $t = 0$. PD parameter estimates and fixed PK parameters are shown in Table 3

describe inflammation and bone destruction in arthritic mice.

Models with a feedback

We denote by $g(s(t), x_1(t), x_2(t))$ the inflow into state $x_1(t)$ depending on $x_1(t)$ and additionally on state $x_2(t)$. This produces a coupling from $x_2(t)$ back to $x_1(t)$ and generates a feedback.

Model C

Model A extended with a feedback reads

$$\begin{aligned} \frac{d}{dt}x_1(t) &= g(s(t), x_1(t), x_2(t)) - k_1x_1(t), \\ x_1(t) &= x_1^0(t) \text{ for } -T \leq t \leq 0 \end{aligned} \quad (54)$$

$$\frac{d}{dt}x_2(t) = k_1x_1(t) - k_1x_1(t - T), \quad x_2(0) = x_2^0. \quad (55)$$

For the schematic of model C see Fig. 8. Due to the coupling of Eqs. (54)–(55) the second equation could not be solved a posteriori.

This structure coincides with the lifespan based tumor growth model presented in Example 2. In this example, the apoptotic cells $x_2(t)$ influence the growth of the tumor, compare Eq. (35). Also note that in Example 2 the rate k_1 is time dependent, i.e. describes the drug-effect term.

Model D

Finally, model B extended with a feedback reads

$$\begin{aligned} \frac{d}{dt}x_1(t) &= g(s(t), x_1(t), x_2(t)) - k_1x_1(t), \\ x_1(t) &= x_1^0(t) \text{ for } -T \leq t \leq 0 \end{aligned} \quad (56)$$

$$\frac{d}{dt}x_2(t) = k_1x_1(t - T) - k_2x_2(t), \quad x_2(0) = x_2^0. \quad (57)$$

The schematic of model D is presented in Fig. 8. We remark that in PKPD also models with a delayed feedback were applied, see e.g. [41]. An example of a cytokine mediated negative feedback in the model of influenza A (Example 5) will discuss this mechanism further.

Example 5: Influenza A virus kinetics

As an example for the application of model D we consider Baccam et al. [42] who developed a model for the kinetics of influenza A virus infection in humans. Let $U(t)$ describe the number of uninfected target cells and $V(t)$ the infectious viral titer of nasal wash. The productively infected cells are divided into infected cells $I_1(t)$ which are yet not able to produce virus and cells $I_2(t)$ actively producing virus. The delay between $I_1(t)$ and $I_2(t)$ cell pools is modeled by a transit compartment approach. It is assumed that the cytokines $F(t)$ (interferons α and β) are secreted from virus-producing cells $I_2(t)$, starting some time after cells begin producing virus, and influence the rate at which infected cells move into the virus producing state. This delay is described by an explicit delay parameter T . The influenza A model reads

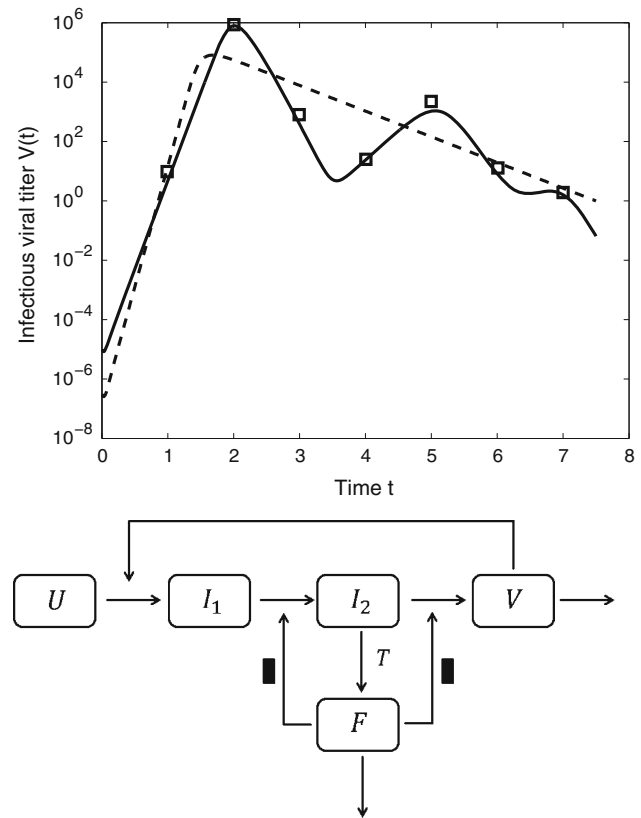


Fig. 10 The dashed line is the infectious viral titer $V(t)$ from the ODE model Eqs. (58)–(61), no interferon effect, and the solid line is $V(t)$ from the DDE model Eqs. (58)–(62) with interferon effect

$$\frac{d}{dt}U(t) = -\beta U(t)V(t), \quad U(0) = U^0 \quad (58)$$

$$\frac{d}{dt}I_1(t) = \beta U(t)V(t) - \frac{kI_1(t)}{1 + \varepsilon_1 F(t)}, \quad I_1(0) = 0 \quad (59)$$

$$\begin{aligned} \frac{d}{dt}I_2(t) &= \frac{kI_1(t)}{1 + \varepsilon_1 F(t)} - \delta I_2(t), \\ I_2(t) &= 0 \text{ for } -T \leq t \leq 0 \end{aligned} \quad (60)$$

$$\frac{d}{dt}V(t) = \frac{pI_2(t)}{1 + \varepsilon_2 F(t)} - cV(t), \quad V(0) = V^0 \quad (61)$$

$$\frac{d}{dt}F(t) = I_2(t - T) - \alpha F(t), \quad F(0) = 0 \quad (62)$$

where β is the infection rate, k a transit rate, δ the rate infected cells die, p the rate the virus increases and c the viral clearance rate. The initial value $U^0 = \frac{c\delta R_0}{p\beta}$ is the number of uninfected target cells where R_0 is a reproductive number and V^0 the initial virus titer. ε_1 and ε_2 are additional transit rates and α is the interferon degradation rate. Eqs. (60) and (62) coincide with model D. In Fig. 10 a fit of the infectious viral titer $V(t)$ and the schematic of Eqs. (58)–(62) is presented. Parameter estimates are shown

Table 4 Parameter estimates for the influenza A model Eqs. (58)–(62) (Example 5) from acslx

Model parameter	Definition	Value ODE	Value DDE (SD)
β	Infection rate constant	$1.1 \text{ E}-3^a$	$2.1 \text{ E}-5^c$
k	Transit rate	$2 \text{ E}0^a$	$48.6 \text{ E}0^b$ (3.27 E0)
δ	Rate infected cells die	$10.9 \text{ E}0^a$	$10.9 \text{ E}0^b$
p	Rate virus increase	$2.1 \text{ E}-2^a$	$1.3 \text{ E}-1^b$ (4.8 E-2)
c	Viral clearance rate	$11 \text{ E}0^a$	$11 \text{ E}0^c$
R^0	Reproductive number	$75 \text{ E}0^a$	$6.4 \text{ E}0^b$ (1.0 E-1)
V^0	Initial virus titer	$3.1 \text{ E}-7^a$	$1 \text{ E}-5^a$
ε_1	Transit rate		$2.7 \text{ E}-3^b$ (8.6 E-4)
ε_2	Transit rate		0^c
α	Interferon degradation rate		$4.7 \text{ E}0^b$ (2.1 E-1)
T	Delay		$1.0 \text{ E}0^b$ (2.3 E-3)

^a Parameter from [42]^b Parameter estimate^c Fixed

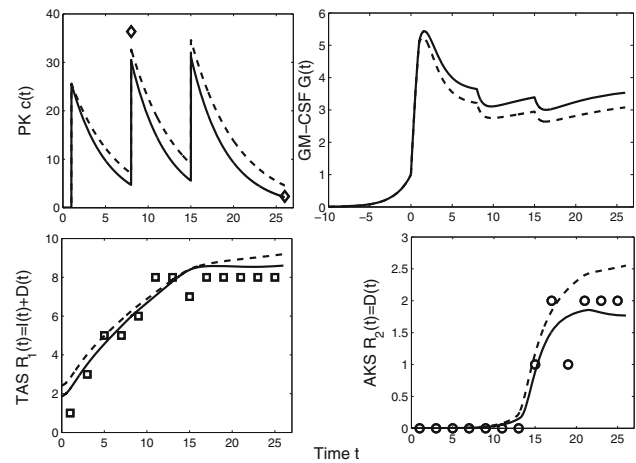
in Table 4. The influenza A model is implemented in acslx and in section “Implementation of delay differential equations” properties of the models are investigated in more detail.

Example 6: A structural combination of model A and B for arthritis development in collagen-induced arthritic mice

In collagen-induced arthritic (CIA) mice increased granulocyte-macrophage colony stimulating factor (GM-CSF) concentration $G(t)$ is inhibited by drug $c(t)$. CIA mice consist of an arthritis induction (no measurements) and an arthritis development (measurements available) phase starting after first visible signs of arthritis. However, it is assumed that the overproduction of the cytokine GM-CSF already appears earlier in the induction phase. A total arthritic score (TAS) $R_1(t)$, an overall description of inflammation $I(t)$ and bone destruction $D(t)$, and an ankylosis score (AKS) $R_2(t)$, describing bone and cartilage destruction of the paws, were measured. The visibility of the ankylosis is strongly delayed due to first signs of inflammation. This delay is described with the structural form of model B. It is assumed that the cytokines drive the inflammation and also the delayed ankylosis. Further it is assumed that the inflammation decreases and runs into a steady state described with model A. The final rheumatoid arthritis (RA) model reads

$$\frac{d}{dt}G(t) = k_3 - \frac{k_1}{k_2}(1 - \exp(-k_2t))G(t) - \frac{E_{\max}c(t)}{EC_{50} + c(t)}G(t),$$

$$G(t) = a \exp(bt) \text{ for } -T \leq t \leq 0 \quad (63)$$



$$\text{Response TAS } R_1(t) = I(t) + D(t)$$

$$\text{Response AKS } R_2(t) = D(t)$$

Fig. 11 A population PKPD analysis with the RA model Eqs. (63)–(67) with 56 mice was performed. The solid line is the response based on the individual parameter and the dashed line is based on the population parameter. We present one individual with dose = 1 at times $t = 1, 8, 15$. In the upper left panel the fit of the sparse PK data is presented and in the upper right panel the prediction for GM-CSF $G(t)$ is plotted. Please note that GM-CSF has a past $[-10, 0]$, compare Eq. (63). In the lower left panel the fit of the TAS $R_1(t)$ is shown and in the lower right panel the fit of the strongly delayed AKS $R_2(t)$ is plotted

$$\frac{d}{dt}I(t) = k_4G(t) - k_4G(t - T), \quad I(0) = I_0 \quad (64)$$

$$\frac{d}{dt}D(t) = k_4G(t - T) - k_5D(t), \quad D(0) = 0 \quad (65)$$

$$R_1(t) = I(t) + D(t) \quad (66)$$

$$R_2(t) = D(t) \quad (67)$$

where k_1, k_2, k_3, a, b are cytokine growth related parameter, k_4 is the production rate of inflammation and k_5 the loss rate of bone destruction. Unlike in the previous models, the RA model has a non-constant past, see Eq. (63), describing the already proliferating cytokines in the arthritis induction phase. We remark that in the presented version of the model the E_{\max} drug effect term was used in contrast to the original model [7]. Nevertheless, the mathematical structure of the model stays untouched.

We implemented the RA model in MONOLIX 4.3, see “Implementation of delay differential equations” section.

Table 5 Population parameter estimates for the RA model Eqs. (63)–(67) (Example 6) from MONOLIX 4.3

Model parameter	Definition	Value (%RSE)
Population		
k	Drug elimination rate	1.84 E–1 (7)
V	Volume of distribution	3.90 E–2 (4)
k_1	Rate constant	5.35 E–1 (10)
k_2	Rate constant	3.52 E–1 (9)
k_3	Rate constant	5 ^a
k_4	Rate constant	1.22 E–1 (12)
k_5	Rate constant	1.26 E–1 (28)
E_{max}	Maximal effect	1 ^a
EC_{50}	Drug concentration yielding half-maximal effect	4.43 E1 (78)
T	Delay of Ankylosis development	1.28 E1 (5)
I_0	Initial value of inflammation	2.42 E0 (14)
a	Parameter for the past of GM-CSF	1 ^a
b	Parameter for the past of GM-CSF	0.5 ^a
BSV		
ω_k^2	Variance	2.12 E–1 (22)
ω_V^2	Variance	4.96 E–3 (>100)
$\omega_{k_1}^2$	Variance	9.70 E–2 (53)
$\omega_{k_2}^2$	Variance	1.37 E–1 (39)
$\omega_{k_3}^2$	Variance	0 ^a
$\omega_{k_4}^2$	Variance	2.79 E–1 (32)
$\omega_{k_5}^2$	Variance	2.15 E0 (28)
$\omega_{E_{max}}^2$	Variance	0 ^a
$\omega_{EC_{50}}^2$	Variance	3.00 E0 ^a
ω_T^2	Variance	7.82 E–2 (26)
$\omega_{I_0}^2$	Variance	5.62 E–1 (30)
ω_a^2	Variance	0 ^a
ω_b^2	Variance	0 ^a
Residual error		
b_1	Proportional error PK	3.82 E–1 (5)
a_2	Additive error TAS	1.49 E0 (2)
a_3	Additive error AKS	4.20 E–1 (4)

The individual parameters are assumed to be log-normal distributed

^a Fixed

The PK $c(t)$ is described with a one-compartment model. In this work we performed a population PKPD analysis of 56 CIA mice in contrast to the original work [7] where mean data was fitted. In Fig. 11 the fit of one individual mouse and the schematic of the RA model Eqs. (63)–(67) are presented. Note the large delay in the development of the AKS which is based on the delayed inflow in Eq. (65). The population parameter estimates are listed in Table 5.

Delay differential equations and mathematical properties

Categories of differential equations

Now we generally describe the pharmacological/biological mechanism by a function f , denoting the right hand side of a rate of change equation, where state x is a vector. Depending on the arguments used in f , different mathematical structures occur. To understand these differences and to motivate the structure of delay differential equations we consider four categories.

Category 1: Pure integration

The first category (C1) is of the form

$$\frac{d}{dt}x(t) = f(t), \quad x(0) = x^0$$

where f is independent of the state $x(t)$. Therefore, we have a pure integration task. E.g. the lifespan model Eq. (16) with an explicit $k_{in}(t)$ and also the precursor lifespan model Eqs. (39)–(40) with an explicit $c(t)$ are of this form.

Category 2: Ordinary differential equations

In the second category (C2), f depends on time t and on the current state $x(t)$. This results in the ordinary differential equation (ODE)

$$\frac{d}{dt}x(t) = f(t, x(t)), \quad x(0) = x^0.$$

PKPD models where the delay is solely modeled by a TCM are of this form.

Category 3: Delay differential equations

In general, in models for biological systems it could be reasonable to include the past of the states into the mechanism f . The delay differential equations (DDE), category 3 (C3), reads

$$\begin{aligned} \frac{d}{dt}x(t) &= f(t, x(t), x(t-T)), \\ x(t) &= x^0(t) \text{ for } -T \leq t \leq 0 \end{aligned} \quad (68)$$

where $T > 0$ is an explicit delay parameter. To highlight the differences between ODEs and DDEs two important features of DDEs are pointed out:

(F1) The mechanism f depends on time t , state $x(t)$ and additionally on the delayed state $x(t-T)$. Thus information from the past is included to describe

the pharmacological mechanism in addition to information contained by the state at present. Therefore, DDEs have an explicit delay parameter $T > 0$ in contrast to ODEs.

- (F2) The initial function $x^0(t)$ describes the past of the state $x(t)$ for $-T \leq t \leq 0$. This allows a description of processes before the actual starting point $t = 0$ of the system.

Note if f does not depend on $x(t - T)$, DDEs reduces to ODEs. Therefore, ODEs are special cases of DDEs. DDEs might generate a more complex time behavior in the solution. Note that in contrast to scalar ODEs, scalar DDEs can produce an oscillating behavior, see Example 8.

The number of delays is not limited to a single delay. With $T_{\max} = \max\{T_1, \dots, T_m\}$ the general form of a DDE consisting of m delays reads

$$\begin{aligned} \frac{d}{dt}x(t) &= f(t, x(t), x(t - T_1), \dots, x(t - T_m)), \\ x(t) &= x^0(t) \text{ for } -T_{\max} \leq t \leq 0. \end{aligned}$$

Category 2.5: Semi-delay differential equations

A special form of delay differential equations reads

$$\frac{d}{dt}x(t) = f(t, x(t)), \quad x(t) = x^0(t) \text{ for } -T \leq t \leq 0 \quad (69)$$

$$\frac{d}{dt}y(t) = g(t, x(t), x(t - T), y(t)), \quad y(0) = y^0 \quad (70)$$

and we call structure Eqs. (69)–(70) semi-DDEs or category 2.5 (C2.5) models. Here the mechanism f does not depend on its delayed state $x(t - T)$. However, $x(t - T)$ is used to describe the mechanism g for $y(t)$ and therefore a past for $x(t)$ is necessary. Note that $y(t)$ has no past but an initial value.

Semi-DDEs/C2.5 models Eqs. (69)–(70) can be simply reformulated as ODEs, see subsection “Writing DDEs as ODEs : The method of steps”, and therefore they can be implemented in PKPD software without a DDE solver, which is a valuable property. Interestingly, many lifespan based PKPD models are of this form, e.g. compare the precursor LIDR Eqs. (48)–(50) from Example 4, the RA model Eqs. (63)–(65) (Example 6) and therefore also models A Eqs. (46)–(47) and B Eqs. (51)–(52). The multiple delay precursor model Eqs. (39)–(40) (Example 3) with an ODE based PK is also of this form, if the Semi-DDE/C2.5 model Eqs. (69)–(70) is formulated for multiple delays.

Example 7: Absorption lag-time

A simplistic way of modeling the absorption delay, see section “Transit compartments for absorption delay”, involves an absorption compartment A_a with an input

delayed by a lag-time T_{lag} . Then the drug is absorbed into the central compartment $A(t)$ at a first order rate k_a :

$$\frac{d}{dt}A_a(t) = Fdose\delta(t - T_{lag}) - k_aA_a(t), \quad A_a(0) = 0 \quad (71)$$

$$\frac{d}{dt}A(t) = k_aA_a(t) - \frac{CL}{V}A(t), \quad A(0) = 0 \quad (72)$$

where the Dirac delta function $\delta(t - T_{lag})$ represents a bolus input $dose$ into the absorption compartment delayed by T_{lag} and F denotes bioavailability. Formally, the one-compartment model with a first-order absorption input with lag-time Eqs. (71)–(72) belongs to category 2. Note that $A(t)$ is equivalent to $\tilde{A}(t)$ from system

$$\begin{aligned} \frac{d}{dt}\tilde{A}_a(t) &= -k_a\tilde{A}_a(t), \\ \tilde{A}_a(t) &= \begin{cases} 0 & \text{for } -T_{lag} \leq t < 0 \\ Fdose & \text{for } t = 0 \end{cases} \end{aligned} \quad (73)$$

$$\frac{d}{dt}\tilde{A}(t) = k_a\tilde{A}_a(t - T_{lag}) - \frac{CL}{V}\tilde{A}(t), \quad \tilde{A}(0) = 0. \quad (74)$$

In Eqs. (73)–(74), the delay appears in the inflow of the central compartment $\tilde{A}(t)$ and Eqs. (73)–(74) is now a C2.5 model.

Example 8: Delayed logistic growth

To further motivate the inclusion of delays into biological systems we follow Arino et al. [43]. The well-known logistic equation describing a population $w(t)$ reads

$$\frac{d}{dt}w(t) = k_g w(t) \left(1 - \frac{w(t)}{w^{ss}}\right), \quad w(0) = w^0 \quad (75)$$

where k_g is the growth rate and $\lim_{t \rightarrow \infty} w(t) = w^{ss}$ is the steady state. If $w(t)$ is small, then the population grows exponentially. In contrast, if $w(t)$ is large, then the individuals of the population compete with each other for the limiting resources and saturation takes place. We emphasize that the solution $w(t)$ of Eq. (75) is strongly monotonic. In the logistic equation it is assumed that the growth rate of the population depends at any time on the number of individuals at that time. However, in practice the process of reproduction is not instantaneous, e.g. due to fertility and therefore, inclusion of delays are necessary. In 1948, Hutchinson [44] proposed the delayed logistic equation

$$\begin{aligned} \frac{d}{dt}w(t) &= k_g w(t) \left(1 - \frac{w(t - T)}{w^{ss}}\right), \quad w(t) = w^0(t) \\ &\text{for } -T \leq t \leq 0 \end{aligned} \quad (76)$$

to model the population of *Daphnia* (a subspecies of Crustaceans) because egg formation occurs T time units before hatching, compare [43]. The delayed logistic growth

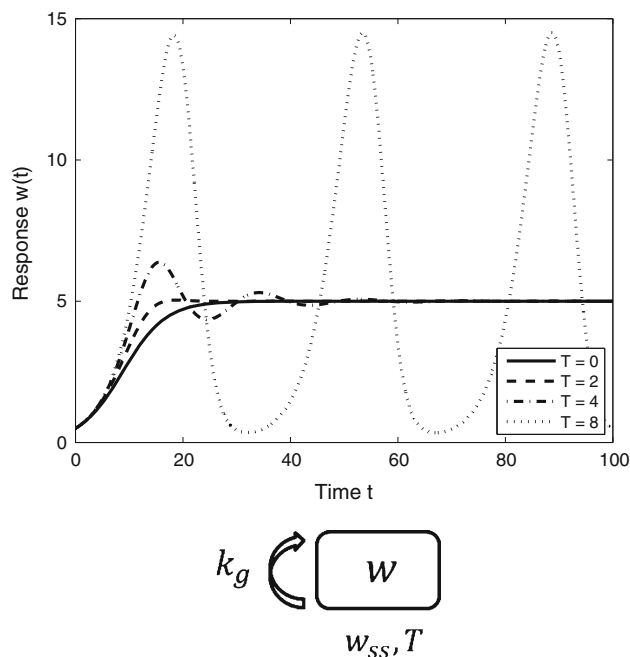


Fig. 12 Delayed logistic growth Eq. (76) with parameter $k_g = 0.25$, $w_0 = 0.5$, $w^{ss} = 5$ and $T \in \{0, 2, 4, 8\}$

is a C3 model. The inclusion of a delay produces a non-monotonic oscillating behavior of the solution $w(t)$. For $kT \in (0, \pi/2)$ these oscillations are damped in time and $w(t)$ runs into the steady state w^{ss} , whereas for $kT > \pi/2$ the solutions converge to a periodic orbit around the steady state w^{ss} (see [45, 46]). Hence, the inclusion of a delay could have enormous impact on the dynamics. In Fig. 12, $w(t)$ for different delays with $w(t) = w^0$ for $t \leq 0$ is plotted and the schematic of Eq. (76) is shown.

Historically, in 1982 Steimer et al. [47] published a two-compartment DDE based PK model for enterohepatic circulation where the flow from the central compartment to peripheral compartment was delayed. Independent of the PKPD context, several models based on DDEs were developed to describe the dynamics of physiological systems. For hematopoiesis see e.g. [48, 49], in context of HIV [50, 51], in the cardiovascular area [52, 53] and for cancer modeling [54, 55].

Writing DDEs as ODEs: The method of steps

DDEs could be rewritten as ODEs by the method of steps (MOS), see [10] or [37]. The idea is to rewrite the DDE as several ODEs for the intervals $[0, T]$, $[T, 2T]$ and so on. Hence, in every step an ODE for a certain interval has to be solved. Unfortunately, after some steps this method results in a large number of ODEs which can be difficult to handle.

We use the MOS to analyze the structure of category 2.5

models Eqs. (69)–(70) and show that this category could be simply rewritten by ODEs, because the number of steps reduces to exactly two steps. However, in general for category 3 models Eq. (68), the number of steps depends on the ratio between the end of the integration interval and the delay, and therefore could become prohibitively large.

Category 2.5: ODE reformulation with MOS

Consider a category 2.5 model:

$$\frac{d}{dt}x(t) = f(t, x(t)), \quad x(t) = x^0(t) \text{ for } -T \leq t \leq 0 \quad (77)$$

$$\frac{d}{dt}y(t) = g(t, x(t), x(t-T), y(t)), \quad y(0) = y^0. \quad (78)$$

Step 1, $0 \leq t \leq T$:

First one substitutes the explicitly known initial function x^0 for the delayed state $x(t-T)$ and obtains the ODE

$$\frac{d}{dt}x(t) = f(t, x(t)), \quad x(0) = x^0(0) \quad (79)$$

$$\frac{d}{dt}y(t) = g(t, x(t), x^0(t-T), y(t)), \quad y(0) = y^0 \quad (80)$$

$$\frac{d}{dt}z(t) = 0 \quad z(0) = x^0(0) \quad (81)$$

where Eq. (81) is a place holder for the upcoming delayed version of Eq. (79).

Step 2, $t \geq T$:

In the second step one duplicates Eq. (79), where z now describes the state of x before $t-T$ time units, i.e. $z(t) = x(t-T)$. We denote by (x^T, y^T) the value of $x(t)$ and $y(t)$ at the time point T . Then the system reads

$$\frac{d}{dt}x(t) = f(t, x(t)), \quad x(T) = x^T \quad (82)$$

$$\frac{d}{dt}y(t) = g(t, x(t), z(t), y(t)), \quad y(T) = y^T \quad (83)$$

$$\frac{d}{dt}z(t) = f(t-T, z(t)), \quad z(T) = x^0(0). \quad (84)$$

Note that we have no more delayed states in the right hand side of Eqs. (82)–(84). Therefore, no further step is necessary and the MOS stops after two steps. We call Eqs. (79)–(81) for $0 \leq t \leq T$ and Eqs. (82)–(84) for $t \geq T$ the category 2.5 ODE formulation (C2.5ODE).

Example 6 (continue): Rheumatoid arthritis model

Consider the RA model which is of C2.5 structure. We exemplarily rewrite the RA model in its C2.5ODE formulation. For $0 \leq t \leq T$ we have

$$\begin{aligned} \frac{d}{dt}G(t) &= k_3 - \frac{k_1}{k_2}(1 - \exp(-k_2t))G(t) \\ &\quad - \frac{E_{\max}c(t)}{EC_{50} + c(t)}G(t), \quad G(0) = a \end{aligned} \quad (85)$$

$$\frac{d}{dt}I(t) = k_4G(t) - k_4a \exp(b(t-T)), \quad I(0) = I_0 \quad (86)$$

$$\frac{d}{dt}D(t) = k_4a \exp(b(t-T)) - k_5D(t), \quad D(0) = 0 \quad (87)$$

$$\frac{d}{dt}z(t) = 0, \quad z(0) = a \quad (88)$$

and for $t \geq T$

$$\begin{aligned} \frac{d}{dt}G(t) &= k_3 - \frac{k_1}{k_2}(1 - \exp(-k_2t))G(t) \\ &\quad - \frac{E_{\max}c(t)}{EC_{50} + c(t)}G(t), \quad G(T) = G^T \end{aligned} \quad (89)$$

$$\frac{d}{dt}I(t) = k_4G(t) - k_4z(t), \quad I(T) = I^T \quad (90)$$

$$\frac{d}{dt}D(t) = k_4z(t) - k_5D(t), \quad D(T) = D^T \quad (91)$$

$$\begin{aligned} \frac{d}{dt}z(t) &= k_3 - \frac{k_1}{k_2}(1 - \exp(-k_2(t-T)))z(t) \\ &\quad - \frac{E_{\max}c(t-T)}{EC_{50} + c(t-T)}z(t), \quad z(T) = a \end{aligned} \quad (92)$$

where (G^T, I^T, D^T, z^T) are the values of the states at time T .

Please note that in Eqs. (85)–(88) for $0 \leq t \leq T$ the delay appears in the explicitly known substituted initial function, whereas, in Eqs. (89)–(92) the delay is now in the PK of the delayed equation $z(t) = G(t-T)$ for $t \geq T$. This is a valuable property for the implementation in PKPD software without a DDE solver.

Example 2 (continue): Lifespan based tumor growth model

The tumor growth model in lifespan formulation Eqs. (31)–(34) is of the form of model C which is of category 3. Therefore, a reformulation in two steps is not possible and the number of steps depends on the ratio between the end of integration and the delay.

Implementation of delay differential equations

Introduction

In general, delay differential equations have to be numerically solved with a DDE solver. Such solvers are an extension of ODE solvers, see e.g. [56, 57]. Currently, no DDE solver is implemented in the PKPD software ADAPT 5 [58], NONMEM 7.2 [59] and PHOENIX 1.3/

WINNONLIN 5 CLASSIC [61]. Nevertheless, we present in this section how different functionalities of PKPD software could be exploited in order to implement Semi-DDE/C2.5 models. In contrast, MONOLIX 4.3 [60] is equipped with a DDE solver and also the general engineering software MATLAB [62] has a DDE solver [63]. In S-ADAPT, [64] a method of step based DDE solver [65] was implemented. Additionally, we remark that BERKELEY MADONNA [66] as well as acslX [67] are able to solve DDEs. Please note that the content of this section reflects the current software situation when this manuscript was published. All presented source codes are available as supplementary material.

PKPD software functionality to solve C2.5/Semi-DDE models

Typically, PKPD software possess of a lag-time feature traditionally used to delay the drug concentration due to absorption effects by shifting the drug concentration $c(t)$ in time for a lag-time T . This software feature will be exploited to implement C2.5 PKPD models. As presented in “Writing DDEs as ODEs: the method of steps” section, the general idea is to duplicate the differential equations which consists of a delay and to apply the lag-time feature to shift the duplicates in time. More precisely, we have one differential equation system running at time t and the other running at time $t-T$. Depending on the complexity of the model, a case-by-case analysis may be necessary in the code as presented for the general C2.5ODE formulation Eqs. (79)–(84) of C2.5 Eqs. (77)–(78).

NONMEM: The ALAG n command

In NONMEM the administration of *dose* via the AMT column in the data file could be shifted with the ALAG n command for any ODE, see [37]. E.g. for a one-compartment model

$$\frac{d}{dt}x_1(t) = -k_{el}x_1(t), \quad x_1(0) = x_1^0 \geq 0 \quad (93)$$

one obtains with ALAG1 = T and *dose* = 10 by the corresponding data set

#ID	TIME	AMT	CMT	DV
1	0	10	1	.

the following behavior.

$$\text{For } 0 \leq t < T: \frac{d}{dt}x_1(t) = -k_{el}x_1(t), \quad x_1(0) = x_1^0 \quad (94)$$

and

$$\text{For } t \geq T: \frac{d}{dt}x_1(t) = -k_{el}x_1(t), \quad x_1(T) = x_1^T + \text{dose}. \quad (95)$$

PHOENIX 1.3: The TLAG command in PML

In PML from PHOENIX the lag-time feature is implemented by the `tlag` option and could be used for any ODE. In case of the one-compartment model Eq. (93) where *dose* is given via the internal dosing function the code reads:

```
deriv(x = -kel * x)
dosepoint(x, tlag = T)
sequence{x = x0}
```

This code produces the same output as Eqs. (94)–(95).

ADAPT 5

C2.5 models, where the delay appears in the PK $c(t)$, could be implemented in ADAPT 5. However, for that the PK and the multiple dosing has to be explicitly coded by the user, see e.g. [68].

WINNONLIN 5 CLASSIC

Similar to ADAPT 5, C2.5 models with the delay in the PK could be implemented with a multiple dosing algorithm provided by the user.

*Software for solving C3/DDE models**MONOLIX 4.3: The delay command in MLXTRAN*

MONOLIX 4.3 provides the command `delay(xi, T)` where *xi* is a one-dimensional component and *T* is the explicit delay. Therefore, DDEs of category 3 with a non-constant past

$$\frac{d}{dt}x(t) = f(x(t), x(t - T)), \quad (96)$$

$$x(t) = x^0(t) \text{ for } -T \leq t \leq 0 \quad (97)$$

could be solved.

BERKELEY MADONNA: The delay command

BERKELEY MADONNA provides the command `delay(xi, T)` where *xi* is a one-dimensional component and *T* is the explicit delay. On the one hand with this command DDEs of category 3 could be solved. However, to implement a non-constant past, $x(t) = x^0(t)$ for $-T \leq t \leq 0$, this past has to be substituted in Eq. (96) for $x(t - T)$ for $0 \leq t \leq T$. Then for $t > T$ the `delay` command is used. This requires a case-by-case analysis of the right hand side in the code. The idea of this method is

demonstrated in Example 9. On the other hand the command could also be used to shift the solution $x(t)$ of

$$\frac{d}{dt}x(t) = f(x(t)), \quad x(0) = x^0$$

in time as follows:

$$x(t) = \begin{cases} x^0 & \text{for } 0 \leq t \leq T \\ x(t - T) & \text{for } t > T \end{cases}.$$

acslX: The delay command

`acslX` provides the command `delay(xi, xi0, T, nmX)` where *xi* is a one-dimensional component, *xi0* is the initial value, *T* is the explicit delay and *nmX* is an integer which allocates space for storing the history data. The properties of `delay` are equal to those of the `delay` command in BERKELEY MADONNA. As explained for BERKELEY MADONNA also a non-constant past could be handled in `acslX`.

S-ADAPT: The XD function

In S-ADAPT, function $XD(i, j)$ represents the *i*th element of the vector x , $x(i)$ delayed by the time $TD(j)$, that is, the *j*th element of the user provided vector of delay times TD , more precisely

$$XD(i, j) = x_i(t - T_j).$$

For example, to delay variable x_1 from model A in Eq. (47) by the delay time *T*, one needs these parts of the code:

$$\begin{aligned} TD(1) &= P(1) \\ XP(2) &= k_1 * X(1) - k_1 * XD(1, 1) \end{aligned}$$

The XD function is part of the S-ADAPT DDE library. As explained for BERKELEY MADONNA a non-constant past could be handled.

MATLAB: The dde23 solver

The `dde23` solver [63] expects a function containing the model of the form

$$\text{function } dx = \text{name}(t, x, z)$$

where vector x contains the states $x(t)$ and matrix z describes the delayed states, more precisely, the elements are $z_{ij} = x_i(t - T_j)$. The past is given via an additional function

$$\text{function } \text{past} = \text{name_hist}(t)$$

where `past` is the vector describing the states $x(t)$ for $t \leq 0$.

Examples

In this section we discuss the implementation of the introduced models in different PKPD software and also present based on the basic LSM Eqs. (22)–(23) a detailed step-by-step analysis.

Example 1 (continue): Basic lifespan model

The basic LSM Eqs. (22)–(23) reads

$$\frac{d}{dt}c(t) = -k_{el}c(t), \quad c(t) = \begin{cases} 0 & \text{for } -T_R \leq t < 0 \\ c^0 \geq 0 & \text{for } t = 0 \end{cases} \quad (98)$$

$$\begin{aligned} \frac{d}{dt}R(t) = k_0 \left(1 + \frac{S_{max}c(t)}{SC_{50} + c(t)} \right) \\ - k_0 \left(1 + \frac{S_{max}c(t - T_R)}{SC_{50} + c(t - T_R)} \right), \quad R(0) = k_0 T_R. \end{aligned} \quad (99)$$

First of all we remark that the right hand side of Eq. (99) is independent of $R(t)$ and $R(t - T_R)$, and that we have a constant past in Eq. (98). Depending on the representation of the PK $c(t)$, one obtains two different mathematical scenarios. For Eq. (99) with an explicit PK representation

$$c(t) = \begin{cases} 0 & \text{for } -T_R \leq t < 0 \\ c^0 \exp(-k_{el}t) & \text{for } t \geq 0 \end{cases} \quad (100)$$

we have a C1 model and therefore Eqs. (99)–(100) could be simply implemented in any PKPD software. In Appendix 1 we present the implementation in WINNONLIN 5 CLASSIC. However, multiple dosing for Eq. (100) has to be coded by the user.

In contrast, Eqs. (98)–(99) form a C2.5 model which could be reformulated by the MOS in two steps. The C2.5ODE version reads for $0 \leq t \leq T_R$

$$\frac{d}{dt}c(t) = -k_{el}c(t), \quad c(0) = c^0 \quad (101)$$

$$\frac{d}{dt}c_{del}(t) = 0, \quad c_{del}(0) = c^0 \quad (102)$$

$$\frac{d}{dt}R(t) = k_0 \left(1 + \frac{S_{max}c(t)}{SC_{50} + c(t)} \right) - k_0, \quad R(0) = k_0 T_R \quad (103)$$

and for $t \geq T_R$

$$\frac{d}{dt}c(t) = -k_{el}c(t), \quad c(T_R) = c^{T_R} \quad (104)$$

$$\frac{d}{dt}c_{del}(t) = -k_{el}c_{del}(t), \quad c_{del}(T_R) = c^0 \quad (105)$$

$$\begin{aligned} \frac{d}{dt}R(t) = k_0 \left(1 + \frac{S_{max}c(t)}{SC_{50} + c(t)} \right) \\ - k_0 \left(1 + \frac{S_{max}c_{del}(t)}{SC_{50} + c_{del}(t)} \right), \quad R(T_R) = R^{T_R}. \end{aligned} \quad (106)$$

Due to the property Eqs. (94)–(95) of ALAG and TLAG no distinction of the right hand side is necessary in the code. In Appendix 1 the implementations in PHOENIX 6.3 and in NONMEM 7.2 are shown. The source code is provided in the supplemental material.

Example 2 (continue): Lifespan based tumor growth model

The lifespan based tumor growth model Eqs. (31)–(34) is of category 3 with a constant past and therefore, a DDE solver is necessary. In Appendix 2 the implementation in BERKELEY MADONNA 8.3 is presented. The source code is provided in the supplemental material.

Example 3 (continue): Precursor lifespan model for platelets

The precursor lifespan model for platelets Eqs. (39)–(40) is implemented in ADAPT 5 with an explicit PK, see Appendix 3. Therefore, Eqs. (39)–(40) reduces to a C1 model. The source code is provided in the supplemental material.

Example 4 (continue): Lifespan indirect response model with a precursor pool

The C2.5 model Eqs. (48)–(50) is implemented in S-ADAPT in its original formulation, see Appendix 4. Additionally, we implemented this model in every PKPD software mentioned in this manuscript. All source codes are provided in the supplemental material.

Example 5 (continue): Influenza A virus kinetics

The influenza A virus model Eqs. (58)–(62) is a C3 model with constant past. However, if $\varepsilon_1 = \varepsilon_2 = 0$ in Eqs. (58)–(62), then the effect of interferon $F(t)$ is turned off and equation Eq. (62) could be omitted, and Eqs. (58)–(61) is a C2 model. For the C2 version we simulated the viral titers $V(t)$ for no interferon effect Eqs. (58)–(61) based on the parameter presented in [42], see Fig. 10, in acslx. Additionally, we fitted the data with an interferon effect Eqs. (58)–(62), see Fig. 10, in acslx software in its DDE formulation, see Appendix 5. The parameters are presented in Table 4. The source code is also provided in the supplemental material.

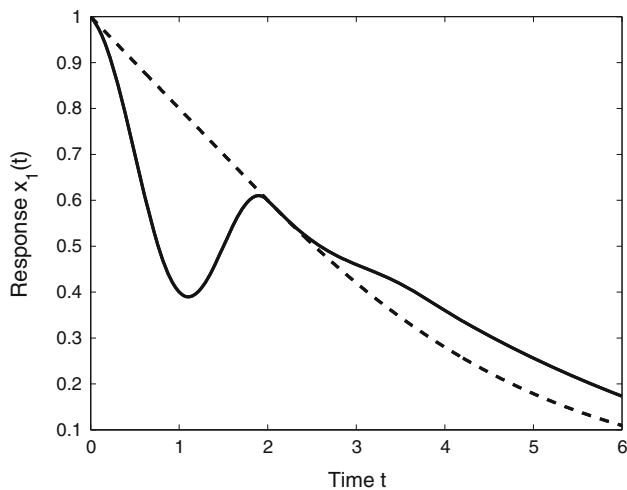


Fig. 13 The dashed line is the simulation of Eq. (107) for constant past ($x_1(t) = 1$ for $-T \leq t \leq 0$) in S-ADAPT. The solid line is the simulation of Eqs. (108)–(109) for non-constant past ($x_1(t) = \pi \sin(\pi t) + 1$ for $-T \leq t \leq 0$) in S-ADAPT. Parameters are $T = 2$ and $k_{el} = 0.2$

Example 6 (continue): Rheumatoid arthritis model

The RA model Eqs. (85)–(92) is implemented in MLXTRAN for MONOLIX 4.3 based on its original C2.5 formulation Eqs. (63)–(67), see Appendix 6. The source code, without the data set, is provided in the supplemental material.

Example 8 (continue): Delayed logistic growth

The delayed logistic growth Eq. (76), a C3 model, is implemented in MATLAB, see Appendix 7. The source code is provided in the supplemental material.

Example 9: Implementation of a non-constant past in S-ADAPT

Consider

$$\frac{d}{dt}x_1(t) = -k_{el}x_1(t - T), \quad x_1(t) = x_1^0(t) \text{ for } -T \leq t \leq 0 \quad (107)$$

where $x_1^0(t) = 1$ (constant past) or $x_1^0(t) = \pi \sin(t\pi) + 1$ (non-constant past) for $-T \leq t \leq 0$. For the non-constant past we implement Eq. (107) as follows:

$$0 \leq t \leq T: \quad \frac{d}{dt}x_1(t) = -k_{el}\pi \sin((t - T)\pi + 1), \quad (108)$$

$$x_1(0) = x_1^0(0)$$

$$t \geq T: \quad \frac{d}{dt}x_1(t) = -k_{el}x_1(t - T), \quad x_1(T) = x_1^T \quad (109)$$

see Appendix 8 for S-ADAPT code. In Fig. 13, the solution for constant and non-constant past are plotted. The source code is provided in the supplemental material.

Discussion

PKPD is a field where delays are omnipresent and we believe that additional mathematical tools could support and improve the PKPD modeling process. At the beginning of this manuscript, we gave a short survey of TCMs to describe delays or aging processes. Undoubtedly, the success of TCMs in PKPD modeling is due to its straightforward structure of the ODE system defining these models. We presented LSMs with either a point distributed or an arbitrary distributed lifespan. Based on LSMs we categorized four basic models which often serve as subunits for more complex models. LSMs also gave us the link to introduce DDEs which are extensions of ODEs because the right hand side of the rate of change equation additionally depends on the delayed states with explicit delay parameters. Also, a past describing the states in an explicit manner before the start of the system is now included in the model. We defined a special subclass of DDEs, the so-called category 2.5 models or semi-DDEs. This category could be simply rewritten as ODEs by the method of steps in two steps. Interestingly, several DDE based PKPD models are of this subclass and could therefore be solved with standard PKPD solvers. However, for general DDEs a numerical DDE solver is necessary which is currently not implemented in every PKPD software.

It is important to point out, if DDEs are applied, the TCM approach could still be used as demonstrated in Example 5. However, be aware of the following fundamental difference between DDEs and ODEs with TCMs. Any delay modeled via a TCM of length n enlarges the number of ordinary differential equations by n , whereas modeling a new delay in the DDE fashion only enlarges the number of dependencies of f by one and the dimension of the resulting system remains unchanged.

Although the difference between ODE and DDE systems is the presence of a delayed state in the differential equation describing the change of state with time, fundamentally these are examples of dynamical systems [70]. A state at a fixed time point t in the sense of dynamical systems is the collection of information which is necessary at time t to let the system uniquely evolve. In this context, DDE based PKPD models are natural extensions of standard ones which differ only by the presence of the past in the evolution of the state. Hereditary systems (dynamical systems with states dependent on the past) have been applied in mathematical modeling for decades [71]. Therefore, one of the goals of this tutorial is to popularize their use in PKPD modeling area.

Unfortunately, at the moment some major PKPD programs do not support DDEs. However, we demonstrated that lag-time functionality, typically implemented in PKPD software, could be utilized to solve C2.5 models. Nevertheless, a numerical DDE solver would be desirable to overcome this software shortcoming in order to exploit the additional properties of general DDE based models for PKPD analysis.

Finally, an interesting extension of the presented DDEs in this manuscript are systems where the delay is not only a value or parameter but modeled via a function incorporating additional dependencies. Such an approach could e.g. be used, if a drug directly affects the lifespan/delay.

For further reading on applications of DDEs to model biological systems and numerical as well as theoretical considerations we refer to the books from Marchuk et al. [72], Smith [73], Driver [10], Kuang [74], Erneux [75], Gopalsamy [76] and Balachandran et al. [77].

Acknowledgments We thank the members of the Buffalo discussion groups from Drs. William J. Jusko and Wojciech Krzyzanski for their fruitful comments. We also thank Drs. Robert Bauer, David D'Argenio, Serge Guzy, Marc Lavielle and Robin McDougall for their valuable input. The present Project is supported by the National Research Fund, Luxembourg, and cofunded under the Marie Curie Actions of the European Commission (FP7-COFUND) (G.K.) and supported in part by NIH Grant GM57980 (W.K.).

Appendix 1

PHOENIX 1.3, WINONLIN 5 CLASSICAL and NONMEM 7.2 codes for Example 1 (Basic lifespan model)

We denote by T the time t and by Tau the delay T in the following codes.

WINNONLIN 5 CLASSICAL source code for model Eqs. (99)–(100):

```
MODEL BasicLSM
COMMANDS
NFUNCTIONS 1
NPARAMETERS 4
PNames 'Smax', 'SC50', 'k0', 'Tau'
NDERIVATIVES 1
END
TEMPORARY
T = X
kel = 0.2
dose = 10
V = 1
END
```

```
START
Z(1) = k0*Tau
END
DIFFERENTIAL
IF T >= 0 THEN
c = dose/V*exp(-kel*T)
ELSE
c = 0
ENDIF
IF T >= Tau THEN
cdel = dose/V*exp(-kel*(T-Tau))
ELSE
cdel = 0
ENDIF
kin = k0*(1+(Smax*c)/(SC50+c))
kindel = k0*(1+(Smax*cdel)/(SC50+cdel))
DZ(1) = kin - kindel
END
FUNCTION 1
F = Z(1)
END
EOM
```

PHOENIX 6.3 PML source code for model Eqs. (101)–(106):

```
LSM_PHX(){
deriv(A = -kel*A)
deriv(Adel = -kel*Adel)
deriv(R = kin-kindel)
dosepoint(A)
dosepoint(Adel, tlag=Tau)
sequence{R = k0*Tau}
c = A/V
cdel = Adel/V
kin = k0*(1+Smax*c/(SC50+c))
kindel = k0*(1+Smax*cdel/(SC50+cdel))
error(REps = 1)
observe(RObs = R*(1+ REps))
stparm(Smax=tvSmax, SC50=tvSC50, k0=tvk0, Tau=tvTau)
stparm(V = 1, kel = 0.2)
fixef(tvSmax = c(0,1,10))
fixef(tvSC50 = c(0,5,50))
fixef(tvk0 = c(0,2,10))
fixef(tvTau = c(0,5,50))
}
```


NONMEM 7.2 source code for model Eqs. (101)–(106):

```

$PROB BasicLSM
$INPUT ID TIME AMT CMT DV
$DATA data_BasicLSM.txt IGNORE #
$SUB
ADVAN13 TOL=8
$MODEL
COMP = (Comp1)
COMP = (Comp2)
COMP = (Comp3)
$PK
kel = Theta(1)
V = Theta(2)
Smax = Theta(3)
SC50 = Theta(4)
k0 = Theta(5)
Tau = Theta(6)
ALAG2 = Tau
A_0(3) = k0*Tau
$DES
DADT(1) = -kel*A(1)
DADT(2) = -kel*A(2)
c = A(1)/V
cdel = A(2)/V
kin = k0*(1+(Smax*c)/(SC50+c))
kindel = k0*(1+(Smax*cdel)/(SC50+cdel))
DADT(3) = kin-kindel
$ERROR
PRED = A(3)
Y = PRED*(1+err(1))
$THETA
0.2 FIX
1 FIX
(0, 1, 10)
(0, 5, 50)
(0, 2, 10)
(0, 5, 50)
$OMEGA
0.01
$EST METHOD = 0 NSIG=8 MAXEVAL=9999 NOABORT PRINT = 1
$TABLE ID TIME FILE=xptab1

```

NONMEM 7.2 data set (fragment):

```

#ID TIME AMT CMT DV
1 0 10 1 .
1 0 10 2 .
1 0 0 3 10
1 1 0 3 11.288
...

```

Appendix 2

Berkeley Madonna code for Example 2 (Lifespan based tumor growth model)

```

method stiff
starttime = 0
stoptime = 25
dtmin = 1e-6
dtmax = 1
tolerance = 1e-6
dt = 1e-6
dose = 100
ka = 103.96*24
ke = 0.1052*24
V = 2.7882
l0 = 0.195
l1 = 0.245
w0 = 0.010
kpot = 0.007
tau = 3.61
init x1 = 0
init x2 = 0
init x3 = w0
init x4 = w0
init x5 = 0
input = pulse(dose,12,1)-pulse(dose,17,1)
d/dt(x1) = input - ka*x1
d/dt(x2) = ka*x1 - ke*x2
c = x2/V
cdel = delay(x2,tau)/V
d/dt(x3) = (2*l0*l1*x3)/(l1+2*l0*x3)
d/dt(x4) = (2*l0*l1*x42)/((l1+2*l0*x4)*(x4+x5))
- kpot*c*x4
d/dt(x5) = kpot*c*x4 - kpot*cdel*delay(x4,tau)
w = x4+x5
display x3,w
display l0,l1,w0,kpot,tau

```

Appendix 3

ADAPT 5 code for Example 3 (Precursor lifespan model for platelets)

We only present the new and modified subroutines from the ADAPT 5 code. For the complete code see supplemental material.

Subroutine SYMBOL:

```

Subroutine SYMBOL
Implicit None
Include 'globals.inc'
Include 'model.inc'
NDEqs = 1
NSParam = 7
NVparam = 1
NSecPar = 0
NSecOut = 0
Ieqsol = 1
Descr = 'Example 3 - PreLSM'
Psym(1) = 'Smax'
Psym(2) = 'SC50'
Psym(3) = 'h'
Psym(4) = 'kin0'
Psym(5) = 'T1'
Psym(6) = 'T2'
Psym(7) = 'eta'
PVsym(1) = 'SDslope1'
Return
End

```

Subroutine for the explicit PK:

```

Subroutine calcPK(c,t)
Implicit none
Real*8 c,t,c1,c2,l1,l2
c1 = 33.08
c2 = 9.266
l1 = 0.1498
l2 = 0.0297
if (t .GE. 0) then
c = c1*exp(-l1*t)+c2*exp(-l2*t)
else
c = 0
end if
Return
End

```

Subroutine DIFFEQ:

```

Subroutine DIFFEQ(T,X,XP)
Implicit None
Include 'globals.inc'
Include 'model.inc'
Real*8 T,X(MaxNDE),XP(MaxNDE)
Real*8 Smax,SC50,h,kin0,T1,T2,eta
Real*8 cdel1,cdel2,kindel1,kindel2
Smax = P(1)
SC50 = P(2)
h = P(3)
kin0 = P(4)
T1 = P(5)
T2 = P(6)
eta = P(7)
call calcPK(cdel1,t-T1)
call calcPK(cdel2,t-T1-T2)
kindel1=eta*kin0*(1+(Smax*cdel1**h)/(SC50**h+cdel1**h))
kindel2=eta*kin0*(1+(Smax*cdel2**h)/(SC50**h+cdel2**h))
XP(1) = kindel1 - kindel2
Return
End

```

Subroutine OUTPUT:

```

Subroutine OUTPUT(Y,T,X)
Implicit None
Include 'globals.inc'
Include 'model.inc'
Real*8 Y(MaxNOE),T,X(MaxNDE)
Y(1) = X(1) + P(7)*P(4)*P(6)
Return
End

```

Subroutine VARMOD:

```

Subroutine VARMOD(V,T,X,Y)
Implicit None
Include 'globals.inc'
Include 'model.inc'
Real*8 V(MaxNOE),T,X(MaxNDE),Y(MaxNOE)
V(1) = (PV(1)*Y(1))**2
Return
End

```

ADAPT 5 data set (fragment):

```
0
0
0
1
21
0 311
24 344
48 373
...
```

ADAPT 5 parameter file (fragment):

```
1 7 2
1.800000
0.100000
1.000000
0.100000
50.00000
...
```

Appendix 4

S-ADAPT code for Example 4 (Lifespan indirect response model with a precursor pool):

We only present the new subroutines for S-ADAPT and skip the unchanged. For the complete code see supplemental material.

Subroutine DEL_DIFFEQ contains the model equations:

```
Subroutine DEL_DIFFEQ(T,X,XP,RD)
Implicit None
Include 'globals.inc'
Include 'model.inc'
Include 'tdelay.inc'
Real*8 T,X(*),XP(*),RD(*)
Real*8 kel,V,k0,k1,Smax,SC50
Real*8 c
TD(1) = P(1)
kel = P(2)
V = P(3)
k0 = P(4)
k1 = P(5)
Smax = P(6)
SC50 = P(7)
c = X(1)/V
XP(1) = -kel*X(1)
XP(2) = k0*(1 + Smax*c/(SC50+c)) - k1*X(2)
XP(3) = k1*X(2) - k1*XD(2,1)
Return
End
```

Subroutine DEL_OUTPUT contains the initial conditions and the output:

```
Subroutine DEL_OUTPUT(Y,T,X)
Implicit None
Include 'globals.inc'
Include 'model.inc'
Include 'tdelay.inc'
Real*8 Y(*),T,X(*)
Real*8 kel,V,k0,k1,Smax,SC50
Real*8 c
NOEQS = 1
TD(1) = P(1)
kel = P(2)
V = P(3)
k0 = P(4)
k1 = P(5)
Smax = P(6)
SC50 = P(7)
X0(1) = 0
X0(2) = k0/k1
X0(3) = k0*TD(1)
Y(1)=log(X(3)+0.0001)
Return
End
```

Subroutine SYMBOL:

```
Subroutine SYMBOL
Implicit None
Include 'globals.inc'
Include 'model.inc'
Include 'tdelay.inc'
character*60 descr
common /descr/ Descr
NDE = 3
NDEL = 1
NDEqs = NDE*(NTD+1)
NSParam = 7
NVparam = 1
Ieqsol = 1
NTPARAM = 5
Descr = 'Example 4 - PreLSM II'
PSYM(1) = 'T'
PSYM(2) = 'kel'
PSYM(3) = 'V'
PSYM(4) = 'k0'
PSYM(5) = 'k1'
PSYM(6) = 'Smax'
PSYM(7) = 'SC50'
PVSYM(1) = 'RESV'
Return
End
```

Subroutine DEL_VARMOD:

```

Subroutine DEL_VARMOD(V,T,X,Y,J)
Implicit None
Include 'globals.inc'
Include 'model.inc'
Include 'tdelay.inc'
Real*8 V(*),T,X(*),Y(*)
V(1) = PV(1)**2
Return
End

```

S-ADAPT data set (fragment):

```

DOSE.DATA
T B(1)
0.00E+00 1000
END
DATA
T Y(1)
0 2.367657649
4 2.971483993
8 4.030494105
12 4.478794243
...
END

```

Appendix 5

acslX code for Example 5 (Influenza A virus kinetics)

```

PROGRAM
DYNAMIC
ALGORITHM IALG = 15
NSTEPS NSTP = 100
MAXTERVAL MAXT = 1
MININTERVAL MINT = 1.0e-9
CINTERVAL CINT = 0.01
CONSTANT TSTOP = 8
DERIVATIVE
constant beta = 1.1e-3
constant k = 2
constant delta = 10.9
constant p = 2.1e-2
constant c = 11
constant R0 = 75
constant V0 = 3.1e-7
constant Tau = 0.5
constant eps1 = 0.001
constant eps2 = 0.001
constant alpha = 2
x10 = (c*delta*R0)/(p*beta)
x20 = 0
x30 = 0
x40 = V0
x50 = 0
x3.del = delay(x3,x30,Tau,100000)
k_new = k/(1+eps1*x5)
p_new = p/(1+eps2*x5)
x1 = integ(-beta*x1*x4,x10)
x2 = integ(beta*x1*x4-k_new*x2,x20)
x3 = integ(k_new*x2-delta*x3,x30)
x4 = integ(p_new*x3-c*x4,x40)
x5 = integ(x3.del-alpha*x5,x50)
END
TERMT (T .GE. TSTOP)
END
END

```

Appendix 6

MONOLIX 4.3 code for Example 6 (Rheumatoid arthritis model)

The MLXTRAN code for MONOLIX 4.3:

```
DESCRIPTION:
RA Model
INPUT:
parameter= {k,V,k1,k2,k3,k4,k5,Emax,EC50,T,I0,a,b}
PK:
compartment(cmt=1, volume=V, concentration=c)
elimination(cmt=1,k)
iv(cmt=1)
EQUATION:
t0 = 0
y1_0 = a*exp(b*t)
y2_0 = I0
y3_0 = 0
eff1 = (Emax*c)/(EC50+c)
ddt_y1 = k3 - eff1*y1 - (k1/k2)*(1-exp(-k2*t))*y1
ddt_y2 = k4*y1 - k4*delay(y1,T)
ddt_y3 = k4*delay(y1,T) - k5*y3
out1 = y2+y3
out2 = y3
OUTPUT:
output = {c,out1,out2}
```

MONOLIX data set (fragment):

```
ID,TIME,AMT,Y,YTYPE,COV
42 1 1 . . 19.24
42 1 . 1 2 19.24
42 1 . 0 3 19.24
42 3 . 3 2 19.24
42 3 . 0 3 19.24
42 5 . 5 2 19.24
42 5 . 0 3 19.24
42 7 . 5 2 19.24
42 7 . 0 3 19.24
42 8 1 . . 19.24
42 8.0033 . 36.34 1 19.24
...
```

Appendix 7

MATLAB code for Example 8 (Delayed logistic growth)

In the first file plot_logistic.m the DDE solver DDE23 is called:

```
clear all;
clear global all;
global g_params;
opt_dde = ddeset('RelTol',1e-8,'AbsTol',1e-8);
k = 0.25;
w0 = 0.5;
wss = 5;
tend = 50;
g_params = [k w0 wss];
delay = 4;
sol = dde23(@fun_logistic_dde,[delay],
    @fun_logistic_dde_hist,[0 tend],opt_dde);
t_plot = sol.x;
y_plot = sol.y;
figure(1); plot(t_plot,y_plot,'black','LineWidth',2);
xlabel('Time t','FontSize',16); ylabel('Response w(t)',
    'FontSize',16); hold on;
```

The second file fun_logistic_dde.m consists of the model:

```
function dx = fun_logistic_dde(t,x,z)
global g_params;
k = g_params(1);
w0 = g_params(2);
wss = g_params(3);
dx(1) = k*x(1)*(1-(z(1,1)/wss));
```

The third file fun_logistic_dde_hist.m contains the past:

```
function erg = fun_logistic_dde_hist(t)
global g_params;
w0 = g_params(2);
erg = w0;
```

Appendix 8

S-ADAPT code for Example 9

We only present the new subroutine DEL_DIFFEQ:

```
Subroutine DEL_DIFFEQ(T,X,XP,RD)
Implicit None
Include 'globals.inc'
Include 'model.inc'
Include 'tdelay.inc'
Real*8 T,X(*),XP(*),RD(*)
Real*8 kel
TD(1) = P(1)
kel = P(2)
if (T.le.TD(1)) then
XP(1) = -kel*(3.1415*sin((T-TD(1))*3.1415)+1)
else
XP(1) = -kel*XD(1,1)
end if
Return
End
```

References

- Mager DE, Wyska E, Jusko WJ (2003) Diversity of mechanism-based pharmacodynamic models. *Drug Metab Dispos* 31:510–519
- Danhof M, De Lange ECM, Della Pasqua OE, Ploeger BA, Voskuyl RA (2008) Mechanism-based pharmacokinetic-pharmacodynamic (PK-PD) modeling in translational drug research. *Trends Pharmacol Sci* 29:186–191
- Savic RM, Jonker DM, Kerbusch T, Karlsson MO (2007) Implementation of a transit compartment model for describing drug absorption in pharmacokinetic studies. *J Pharmacokinet Pharmacodyn* 34:711–726
- Huang W, Lee SL, Yu LX (2009) Mechanistic approach to predicting oral drug absorption. *AAPS J* 11:217–224
- Sheiner LB, Stanski DR, Vozeh S, Miller RD, Ham J (1979) Simultaneous modeling of pharmacokinetics and pharmacodynamics: application to d-tubocurarine. *Clin Pharmacol Ther* 25(3):358–371
- Mager DE, Jusko WJ (2001) Pharmacodynamic modeling of time-dependent transduction systems. *Clin Pharmacol Ther* 70(3):210–216
- Koch G, Wagner T, Plater-Zyberk C, Lahu G, Schropp J (2012) Multi-response model for rheumatoid arthritis based on delay differential equations in collagen-induced arthritic mice treated with an anti-GM-CSF antibody. *J Pharmacokinet Pharmacodyn* 39(1):55–65
- MacDonald N (1978) Time lags in biological models. *Lecture Notes in biomathematics* 27. Springer, Berlin
- Sun YN, Jusko WJ (1998) Transit compartments versus gamma distribution function to model signal transduction processes in pharmacodynamics. *J Pharm Sci* 87(6):732–737
- Driver RD (1977) Ordinary and delay differential equations. *Applied mathematical sciences* 20. Springer, New York
- Lledó-García R, Kalicki RM, Uehlinger DE, Karlsson MO (2012) Modeling of red blood cell life-spans in hematologically normal populations. *J Pharmacokinet Pharmacodyn* 39(5):453–462
- Bischoff KB, Dedrick RL, Zaharko DS, Longstreth JA (1971) Methotrexate pharmacokinetics. *J Pharm Sci* 60(8):1128–1133
- Rousseau A, Léger F, Le Meur Y, Saint-Marcoux F, Paintaud G, Buchler M, Marquet P (2004) Population pharmacokinetic modeling of oral cyclosporin using NONMEM. Comparison of absorption pharmacokinetic models and design of a bayesian estimator. *Ther Drug Monit* 26:23–30
- Shen J, Boeckmann A, Vick A (2012) Implementation of dose superimposition to introduce multiple doses for a mathematical absorption model (transit compartment model). *J Pharmacokinet Pharmacodyn* 39:251–262
- Lobo ED, Balthasar JP (2002) Pharmacodynamic modeling of chemotherapeutic effects: application of a transit compartment model to characterize methotrexate effects in vitro. *AAPS PharmSci* 4(4):E42
- Earp JC, Dubois DC, Molano DS, Pyszczyński NA, Keller CE, Almon RR, Jusko WJ (2008) Modeling corticosteroid effects in a rat model of rheumatoid arthritis I: mechanistic disease progression model for the time course of collagen-induced arthritis in Lewis rats. *J Pharmacol Exp Ther* 326(2):532–545
- Friberg LE, Henningsson A, Maas H, Nguyen L, Karlsson MO (2002) Model of chemotherapy-induced myelosuppression with parameter consistency across drugs. *J Clin Oncol* 20(24):4713–4721
- Dayneka NL, Garg V, Jusko WJ (1993) Comparison of four basic models of indirect pharmacodynamic responses. *J Pharmacokinet Biopharm* 21(4):457–478
- Harker LA, Roskos LK, Marzec UM, Carter RA, Cherry JK, Sundell B, Cheung EN, Terry D, Sheridan W (2000) Effects of megakaryocyte growth and development factor on platelet production, platelet life span, and platelet function in healthy human volunteers. *Blood* 95(8):2514–2522
- Wang YM, Krzyzanski W, Doshi S, Xiao JJ, Pérez-Ruixo JJ, Chow AT (2010) Pharmacodynamics-mediated drug disposition (PDMDD) and precursor pool lifespan model for single dose of romiplostim in healthy subjects. *AAPS J* 12(4):729–740
- Pérez-Ruixo JJ, Krzyzanski W, Hing J (2008) Pharmacodynamic analysis of recombinant human erythropoietin effect on reticulocyte production rate and age distribution in healthy subjects. *Clin Pharmacokinet* 47(6):399–415
- Agoram B, Heatherington AC, Gastonguay MR (2006) Development and evaluation of a population pharmacokinetic-pharmacodynamic model of darbepoetin alfa in patients with nonmyeloid malignancies undergoing multicycle chemotherapy. *AAPS J* 8(3):552–563
- Doshi S, Chow A, Pérez Ruixo JJ (2010) Exposure-response modeling of darbepoetin alfa in anemic patients with chronic kidney disease not receiving dialysis. *J Clin Pharmacol* 50(9):75–90
- Simeoni M, Magni P, Cammia C, De Nicolao G, Croci V, Pesenti E, Germani M, Poggesi I, Rocchetti M (2004) Predictive pharmacokinetic-pharmacodynamic modeling of tumor growth kinetics in xenograft models after administration of anticancer agents. *Cancer Res* 64(3):1094–1101
- Krzyzanski W, Sutjandra L, Pérez-Ruixo JJ, Sloey B, Chow AT, Wang YM (2013) Pharmacokinetic and pharmacodynamic modeling of romiplostim in animals. *Pharm Res* 30(3):655–669
- Bergner PE (1962) On the stochastic interpretation of cell survival curves. *J Theoret Biol* 2(3):279–295
- Krzyzanski W (2011) Interpretation of transit compartments pharmacodynamic models as lifespan based indirect response models. *J Pharmacokinet Pharmacodyn* 38(2):179–204

28. Koch G, Schropp J (2012) General relationship between transit compartments and lifespan models. *J Pharmacokinet Pharmacodyn* 39(4):343–355
29. Krzyzanski W, Ramakrishnan R, Jusko WJ (1999) Basic pharmacodynamic models for agents that alter production of natural cells. *J Pharmacokinet Biopharm* 27(5):467–489
30. Samtani MN, Perez-Ruixo JJ, Brown KH, Cerneus D, Molloy CJ (2009) Pharmacokinetic and pharmacodynamic modeling of pegylated thrombopoietin mimetic peptide (PEG-TPOm) after single intravenous dose administration in healthy subjects. *J Clin Pharmacol* 49(3):336–350
31. Krzyzanski W, Woo S, Jusko WJ (2006) Pharmacodynamic models for agents that alter production of natural cells with various distributions of lifespans. *J Pharmacokinet Pharmacodyn* 33(2):125–166
32. Freise KJ, Widness JA, Schmidt RL, Veng-Pedersen P (2008) Modeling time variant distributions of cellular lifespans: increases in circulating reticulocyte lifespans following double phlebotomies in sheep. *J Pharmacokinet Pharmacodyn* 35(3):285–323
33. Koch G, Schropp J (2013) Solution and implementation of distributed lifespan models. *J Pharmacokinet Pharmacodyn* 40(6):639–650
34. Krzyzanski W, Pérez-Ruixo JJ (2007) An assessment of recombinant human erythropoietin effect on reticulocyte production rate and lifespan distribution in healthy subjects. *Pharm Res* 24(4):758–772
35. Krzyzanski W, Pérez Ruixo JJ, Vermeulen A (2008) Basic pharmacodynamic models for agents that alter the lifespan distribution of natural cells. *J Pharmacokinet Pharmacodyn* 35(3):349–377
36. Krzyzanski W, Pérez Ruixo JJ (2012) Lifespan based indirect response models. *J Pharmacokinet Pharmacodyn* 39(1):109–123
37. Pérez-Ruixo JJ, Kimko HC, Chow AT, Piotrovsky V, Krzyzanski W, Jusko WJ (2005) Population cell life span models for effects of drugs following indirect mechanisms of action. *J Pharmacokinet Pharmacodyn* 32(5–6):767–793
38. Krzyzanski W, Jusko WJ, Wacholtz MC, Minton N, Cheung WK (2005) Pharmacokinetic and pharmacodynamic modeling of recombinant human erythropoietin after multiple subcutaneous doses in healthy subjects. *Eur J Pharm Sci* 26(3–4):295–306
39. Pérez-Ruixo JJ, Krzyzanski W, Bouman-Thio E, Miller B, Jang H, Bai SA, Zhou H, Yohrling J, Cohen A, Burggraaf J, Franson K, Davis HM (2009) Pharmacokinetics and pharmacodynamics of the erythropoietin Mimetic body construct CNTO 528 in healthy subjects. *Clin Pharmacokinet* 48(9):601–613
40. Sharma A, Ebling WF, Jusko WJ (1998) Precursor-dependent indirect pharmacodynamic response model for tolerance and rebound phenomena. *J Pharm Sci* 87:1577–1584
41. Ramakrishnan R, Cheung WK, Wacholtz MC, Minton N, Jusko WJ (2004) Pharmacokinetic and pharmacodynamic modeling of recombinant human erythropoietin after single and multiple doses in healthy volunteers. *J Clin Pharmacol* 44(9):991–1002
42. Baccam P, Beauchemin C, Macken CA, Hayden FG, Perelson A (2006) Kinetics of influenza A virus infection in humans. *J Virol* 80(15):7590–7599
43. Arino O, Hbid ML, Dads Ait E (2006) Delay differential equations and applications. Springer, Berlin
44. Hutchinson GE (1948) Circular causal systems in ecology. *Ann NY Acad Sci* 50:221–246
45. Arino J, Wang L, Wolkowicz GSK (2006) An alternative formulation for a delayed logistic equation. *J Theor Biol* 241:109–119
46. Wright EM (1955) A nonlinear difference-differential equation. *J Reine Angew Math* 494:66–87
47. Steimer JL, Plusquellec Y, Guillaume A, Boisvieux JF (1982) A time-lag model for pharmacokinetics of drugs subject to enterohepatic circulation. *J Pharm Sci* 71(3):297–302
48. Mackey MC, Glass L (1977) Oscillation and chaos in physiological control systems. *Science* 197(4300):287–89
49. Belair J, Mackey MC, Mahaffy JM (1995) Age-structured and two-delay models for erythropoiesis. *Math Biosci* 128(1–2):317–346
50. Culshaw RV, Ruan S (2000) A delay-differential equation model of HIV infection of CD4(+) T-cells. *Math Biosci* 165(1):27–39
51. Bachar M, Dorfmayr A (2004) HIV treatment models with time delay. *C R Biol* 327(11):983–994
52. Fowler AC, McGuinness MJ (2005) A delay recruitment model of the cardiovascular control system. *J Math Biol* 51:508–526
53. Violon D (2012) Kinetics of intravenous radiographic contrast medium injections as used on CT: simulation with time delay differential equations in a basic human cardiovascular multi-compartment model. *Br J Radiol* 85(1020):1212–1218
54. Villasana M, Radunskaia A (2003) A delay differential equation model for tumor growth. *J Math Biol* 47(3):270–294
55. Kim PS, Lee PP (2012) Modeling protective anti-tumor immunity via preventative cancer vaccines using a hybrid agent-based and delay differential equation approach. *PLoS Comput Biol* 8(10):e1002742
56. Hairer E, Nørsett SP, Wanner G (2000) Solving ordinary differential equations I, Second Revised Edition. Springer, Berlin
57. Oberle HJ, Pesch HJ (1981) Numerical treatment of delay differential equations by Hermite interpolation. *Numer Math* 37:235–255
58. D’Argenio DZ, Schumitzky A, Wang X (2009) ADAPT 5 user’s guide: pharmacokinetic/ pharmacodynamic systems analysis software. Biomedical Simulations Resource, Los Angeles
59. Beal S, Sheiner LB, Boeckmann A, Bauer RJ (2009) NONMEM user’s guides. Icon Development Solutions, Ellicott City
60. Lavielle M, Meza H, Chatel K (2014) The monolix software 4.3. Lixoft, Orsay
61. PHOENIX/WINNONLIN 6.3, Pharsight, A Certara Company
62. MATLAB Release (2013a) The MathWorks, Inc. MathWorks, Natick
63. Shampine LF, Thompson S (2001) Solving DDEs in MATLAB. *Appl Numer Math* 37:441–458
64. Bauer RJ (2011) S-ADAPT/MCPEM User’s guide. S-ADAPT Version 1.57, Berkeley, CA, USA
65. Bauer RJ, Mo G, Krzyzanski W (2013) Solving delay differential equations in S-ADAPT by method of steps. *Comput Methods Programs Biomed* 111(3):715–734
66. Macey RI, Oster GF (2010) Berkeley Madonna 8.3. University of California, San Diego
67. acslX, The AEGIS Technologies Group Inc., Huntsville, AL, USA
68. Gibaldi M, Perrier D (1982) Pharmacokinetics, Second Edition Revised and Expanded. Marcel Dekker, New York
69. Krzyzanski W, Wiczling P, Lowe P, Pigeolet E, Fink M, Berghout A, Balser S (2010) Population modeling of filgrastim PK-PD in healthy adults following intravenous and subcutaneous administrations. *J Clin Pharmacol* 50:101–112
70. Hale JK, Lunel SMV (1993) Introduction to functional differential equations. Springer, New York
71. Hale JK, Curz MA (1970) Existence, uniqueness and continuous dependence for hereditary systems. *Ann Mat Pur Appl* 85(1):63–81
72. Marchuk GI (1997) Mathematical modelling of immune response in infectious diseases. Kluwer Academic Publishers, Dordrecht

73. Smith H (2011) An introduction to delay differential equations with applications to the life sciences. Springer, New York
74. Kuang Y (1993) Delay differential equations: with applications in population dynamics. Elsevier, Boston
75. Erneux T (2009) Applied delay differential equations. Springer, New York
76. Gopalsamy K (1992) Stability and oscillations in delay differential equations of population dynamics. Kluwer Academic Publishers, Dordrecht
77. Balachandran B, Kalmár-Nagy T, Gilsinn DE (2009) Delay differential equations: recent advances and new directions. Springer, New York